The nuclear EoS: from experiments to astrophysical observations by the hand of a theoretician

Isaac Vidaña, INFN Catania

International Workshop on Multi facets of EoS & Clustering
22-25 May 2018, Catania (Italy)

In this talk …

I will review different experimental and astrophysical observational constraints of the nuclear EoS as well as some of the phenomenological models & ab-initio theoretical many-body approaches commonly used in its description

Two recent excellent reviews on the topic are

- Oertel, Hempel, Klahn & Typel, Rev. Mod. Phys. 89, 015007 (2017)
- Burgio & Fantina, arXiv:1804.03020 (2018). To appear in the NewCompstar White Book

What do we know to build the nuclear EoS ?

- Masses, radii & other properties of more than 3000 isotopes
- Scattering (cf. > 4000 NN data for $E_{lab} < 350$ MeV)

J. Erler et al., Nature 486, 509 (2012)

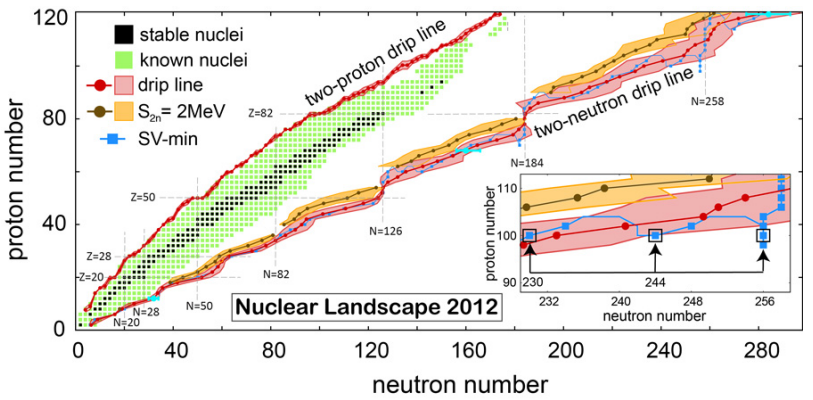

- Around ρ_0 & β=0 the nuclear EoS can be characterized by a few isoscalar (E_0 ,K_0, Q_0) & isovector (E_{sym}, K_{sym}, Q_{sym}) parameters which can be constrained by nuclear experiments & astrophysical observables

$$\frac{E}{A}(\rho,\beta) = E_0 + \frac{1}{2}K_0 x^2 + \frac{1}{6}Q_0 x^3 + \left(E_{sym} + Lx + \frac{1}{2}K_{sym}x^2 + \frac{1}{6}Q_{sym}x^3\right)\beta^2 + \cdots \quad , \quad x = \frac{\rho-\rho_0}{3\rho_0}$$

- Extrapolation to high densities should rely on theoretical models to be tested with astrophysical observations

Constraints from Nuclear Physics Experiments

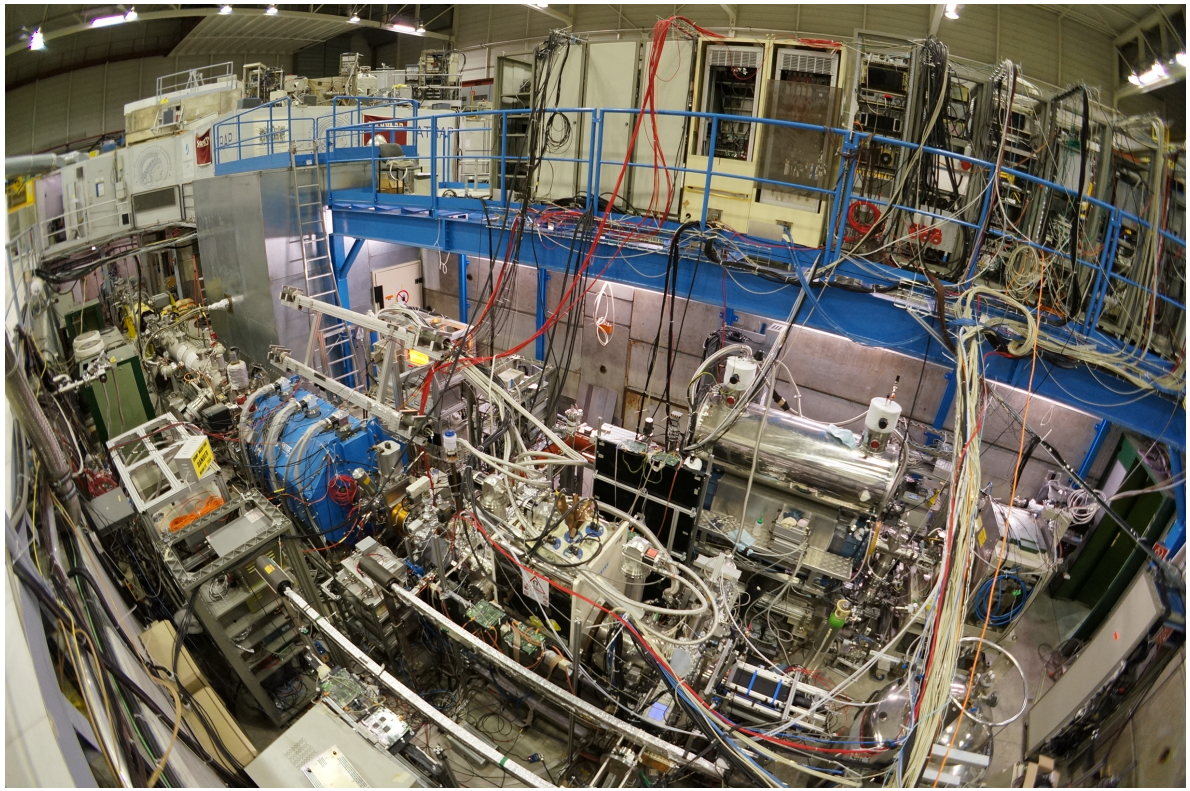

Density Distributions & Nuclear Binding Energies

✧ **Density distributions:**

(e,e') elastic scattering, hadron proves $\xrightarrow{A = N + Z \to \infty}$ $\rho_0 \sim 0.16 \ \ \mathrm{fm}^{-3}$

✧ **Nuclear binding energies:**

$$B(N,Z) = a_v A + a_s A^{2/3} + a_c \frac{Z^2}{A^{1/3}} + \left(a_{Av} A + a_{As} A^{2/3}\right) \frac{(N-Z)^2}{A^2} + \delta a_p A^{-1/2}$$

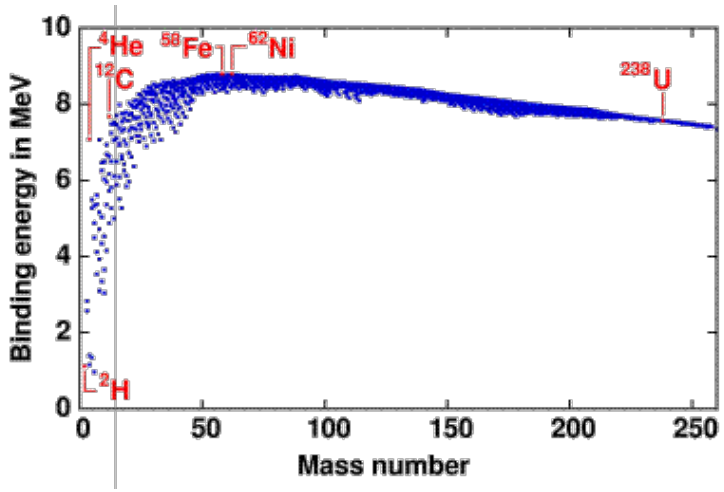

Measurements of nuclear binding energies allow the identification

$$a_V \Leftrightarrow B_{sat} = -E_0$$
$$a_{Av} \Leftrightarrow E_{sym}$$

(in the limit $A = N + Z \to \infty$)

Recent fits of binding energies with non-relativistic & relativistic EDF give

SHF models: $B_{sat} = (15.96 \pm 0.31)$ MeV, $E_{sym} = (31.2 \pm 6.7)$ MeV

RMF models: $B_{sat} = (16.13 \pm 0.51)$ MeV, $E_{sym} = (33.4 \pm 4.7)$ MeV

Dutra et al., PRC 85, 035201 (2012); PRC 90, 055203 (2014)

Nuclear Resonances

ISGMR

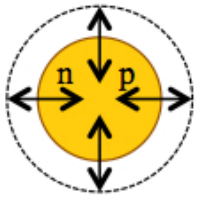

ΔL=0
ΔS=0, ΔT=0

K_0 from the measurement of excitation energy E_{ISGMR}

Typical values in the range ~ 210 – 270 MeV

Phys. Rev. 64, 171 (1980); PRC 90, 055203 (2014)

IVGDR

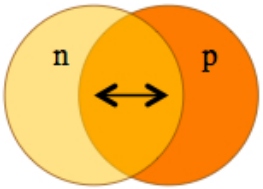

ΔL=1
ΔS=0, ΔT=1

Symmetry energy influences the excitation energies of IVGDR. Their analysis allows to determine E_{sym}

$$23.3 < E_{sym}\left(\rho = 0.1\text{fm}^{-3}\right) = 24.9 \quad \text{MeV}$$

Trippa et al., PRC 77, 061304 (R) (2008)

ISGQR & IVGDR

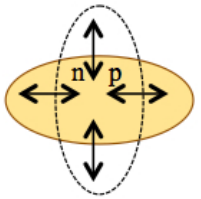

ΔL=2
ΔS=0, ΔT=0

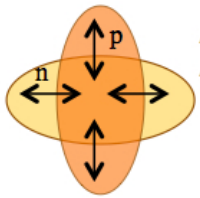

ΔL=2
ΔS=0, ΔT=1

Correlation of Δr_{np} with ISGQR & IVGQR excitation energies from which

$$\Delta\left(^{208}\text{Pb}\right) = 0.14 \pm 0.03 \quad \text{fm}, \qquad L = 37 \pm 18 \quad \text{MeV}$$

Roca-Maza et al., PRC 87, 037301 (2013)

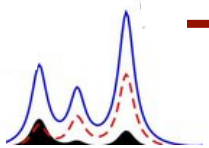

PDR

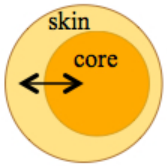

Collective oscillation of neutron skin against the core

Sensitive to the symmetry energy. A recent analysis of PDR in ^{68}Ni & ^{132}Sn using RPA models for the dipole response based in Skyrme & RMF give

$$E_{sym} = 32.3 \pm 1.3 \quad \text{MeV}, \qquad L = \quad 64.8 \pm 15.7 \quad \text{MeV}$$

Carbone et al., PRC 81, 041301 (R) (2010)

Neutron Skin Thickness & Electric Dipole Polarizability

✧ Neutron skin thickness Δr_{np}

Accurate measurements of Δr_{np} via parity-violating electron scattering or antiprotonic atom data can constrain $E_{sym}(\rho)$, particulary L via its strong correlation with Δr_{np}

Viñas et al., EPJA 50, 27 (2014)

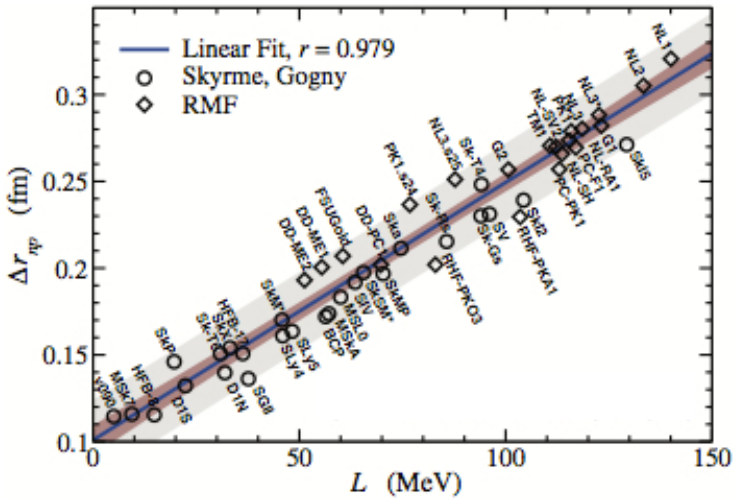

✧ Electric dipole polarizability α_D

Information on $E_{sym}(\rho)$ from available data of α_D of ^{68}Ni, ^{120}Sn & ^{208}Pb. Strong correlation of $\alpha_D E_{sym}$ with L

$$E_{sym} = 30 - 35 \ \text{MeV}, \quad L = 22 - 66 \ \text{MeV}$$

$$\Delta r_{np}(^{68}\text{Ni}) = 0.15 - 0.19 \ \text{fm}$$

$$\Delta r_{np}(^{120}\text{Sn}) = 0.12 - 0.16 \ \text{fm}$$

$$\Delta r_{np}(^{208}\text{Pb}) = 0.13 - 0.19 \ \text{fm}$$

Roca-Maza et al., PRC 92, 064304 (2015)

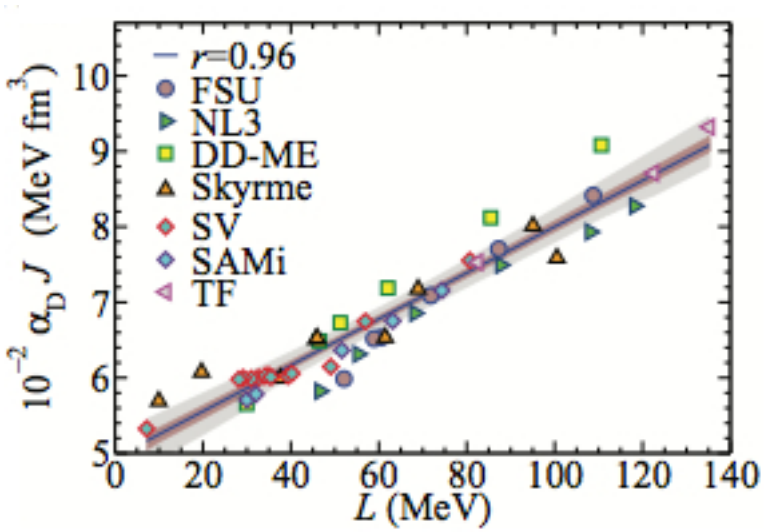

EoS from Heavy Ion Collisions

The analysis of data from HIC requires the use of transport models which do not depend directly on the EoS but rather on the mean field of the participant particles & the in-medium cross sections of the relevant reactions

However, there are several transport codes in the market. A natural question arises: How much the results depend on the transport codes ?

P. Danielewicz et al., Science 298, 1592 (2002)

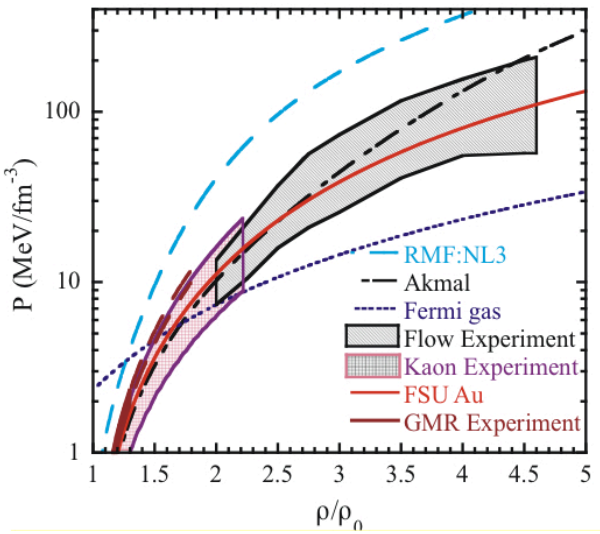

Several observables in HIC are sensitive to the nuclear EoS

sub-saturation densities

- ✓ n/p & t/^{3}He ratios
- ✓ isospin fragmentation & isospin scaling
- ✓ np correlation functions at low rel. mom.
- ✓ isospin difussion/transport
- ✓ neutron-proton differential flow

supra-saturation densities

- ✓ π^-/π^+ & K^-/K^+ ratios
- ✓ np differential transverse flow
- ✓ nucleon elliptic flow at high trans. mom.
- ✓ n/p ratio of squeezed out nucleons perpendicular to the reaction plane

Neutron Skin Thickness & Symmetry Energy from Isobar Charge Exchange Reactions

Accurate measurements of $R = \dfrac{\sigma_{(^{A}Z,^{A}(Z+1))}}{\sigma_{(^{A}Z,^{A}(Z-1))}}$

can be used to extract the neutron skin thickness of heavy nuclei & L

^{136}Xe on a proton target at 1GeV/A

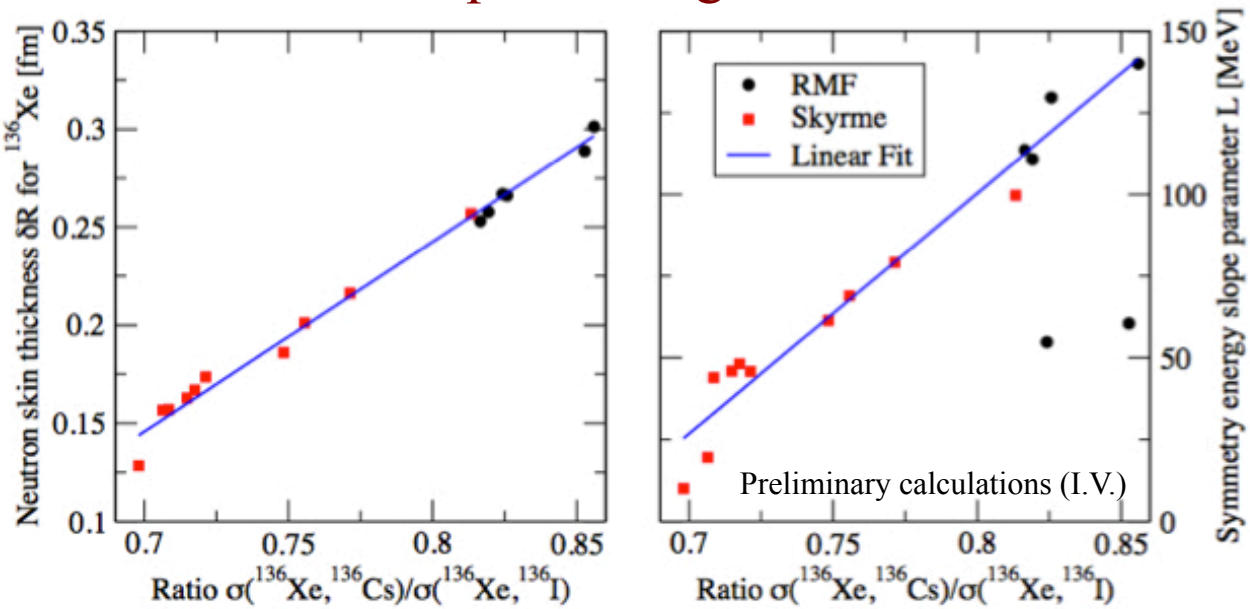

Proposal for SuperFRS. Spokesperson: J. Benlliure

Astrophysical Constraints

Neutron Star Masses

NS masses can be inferred directly from observations of binary systems

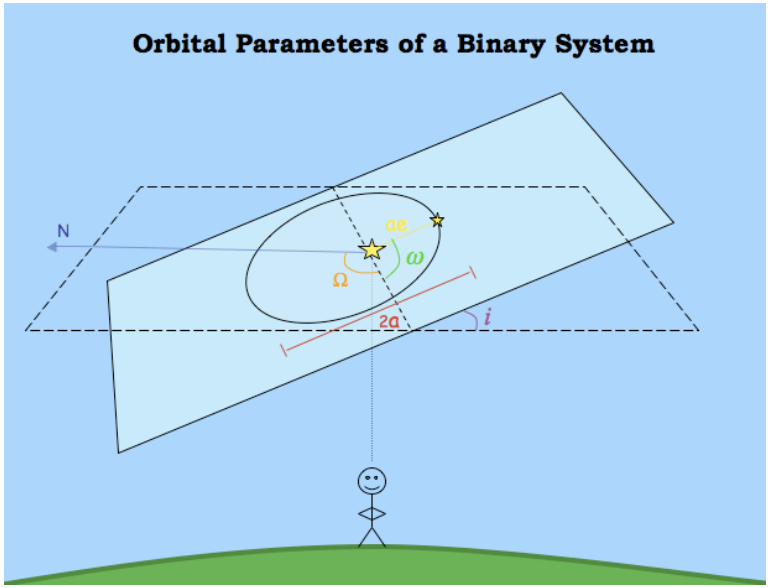

- 5 orbital (Keplerian) parameters can be precisely measured:
  - ✓ Orbital period (P)
  - ✓ Projection of semimajor axis on line of sight (a sin i)
  - ✓ Orbit eccentricity (ε)
  - ✓ Time of periastron (T_0)
  - ✓ Longitude of periastron (ω_0)
- 3 unknowns: M_1, M_2, i

Kepler's 3rd law

$$\frac{G(M_1+M_2)}{a^3}=\left(\frac{2\pi}{P}\right)^2 \rightarrow f(M_1,M_2,i)\equiv\frac{(M_2\sin i)^3}{(M_1+M_2)^2}=\frac{Pv^3}{2\pi G}$$

mass function

In few cases small deviations from Keplerian orbit due to GR effects can be detected

Measure of at least 2 post-Keplerian parameters → High precision NS mass determination

$$\dot{\omega} = 3T_{\odot}^{2/3}\left(\frac{P_b}{2\pi}\right)^{-5/3}\frac{1}{1-\varepsilon}\left(M_p + M_c\right)^{2/3}$$ → Advance of the periastron

$$\gamma = T_{\odot}^{2/3}\left(\frac{P_b}{2\pi}\right)^{1/3}\varepsilon\frac{M_c\left(M_p + 2M_c\right)}{\left(M_p + M_c\right)^{4/3}}$$ → Time dilation & grav. redshift

$$r = T_{\odot}M_c$$ → Shapiro delay "range"

$$s = \sin i = T_{\odot}^{-1/3}\left(\frac{P_b}{2\pi}\right)^{-2/3}x\frac{\left(M_p + M_c\right)^{2/3}}{M_c}$$ → Shapiro delay "shape"

$$\dot{P}_b = -\frac{192\pi}{5}T_{\odot}^{5/3}\left(\frac{P_b}{2\pi}\right)^{-5/3}f(\varepsilon)\frac{M_pM_c}{\left(M_p + M_c\right)^{1/3}}$$ → Orbit decay due to GW emission

Recent Measurements of High NS Masses

- PSR J164-2230 (Demorest et al. 2010)

  - ✓ binary system (P=8.68 d)
  - ✓ low eccentricity ($\varepsilon=1.3 \times 10^{-6}$)
  - ✓ companion mass: $\sim 0.5 M_{\odot}$
  - ✓ pulsar mass: $M = 1.928 \pm 0.017 M_{\odot}$

- PSR J0348+0432 (Antoniadis et al. 2013)

  - ✓ binary system (P=2.46 h)
  - ✓ very low eccentricity
  - ✓ companion mass: $0.172 \pm 0.003 M_{\odot}$
  - ✓ pulsar mass: $M = 2.01 \pm 0.04 M_{\odot}$

In this decade NS with $2M_{\odot}$ have been observed by measuring post-Keplerian parameters of their orbits

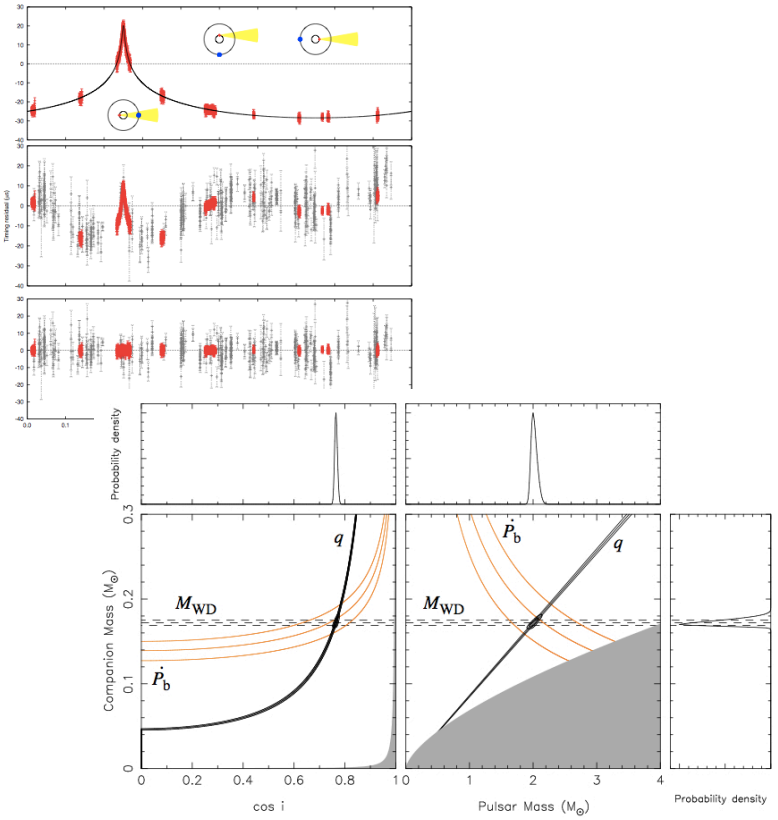

Measured Neutron Star Masses (2018)

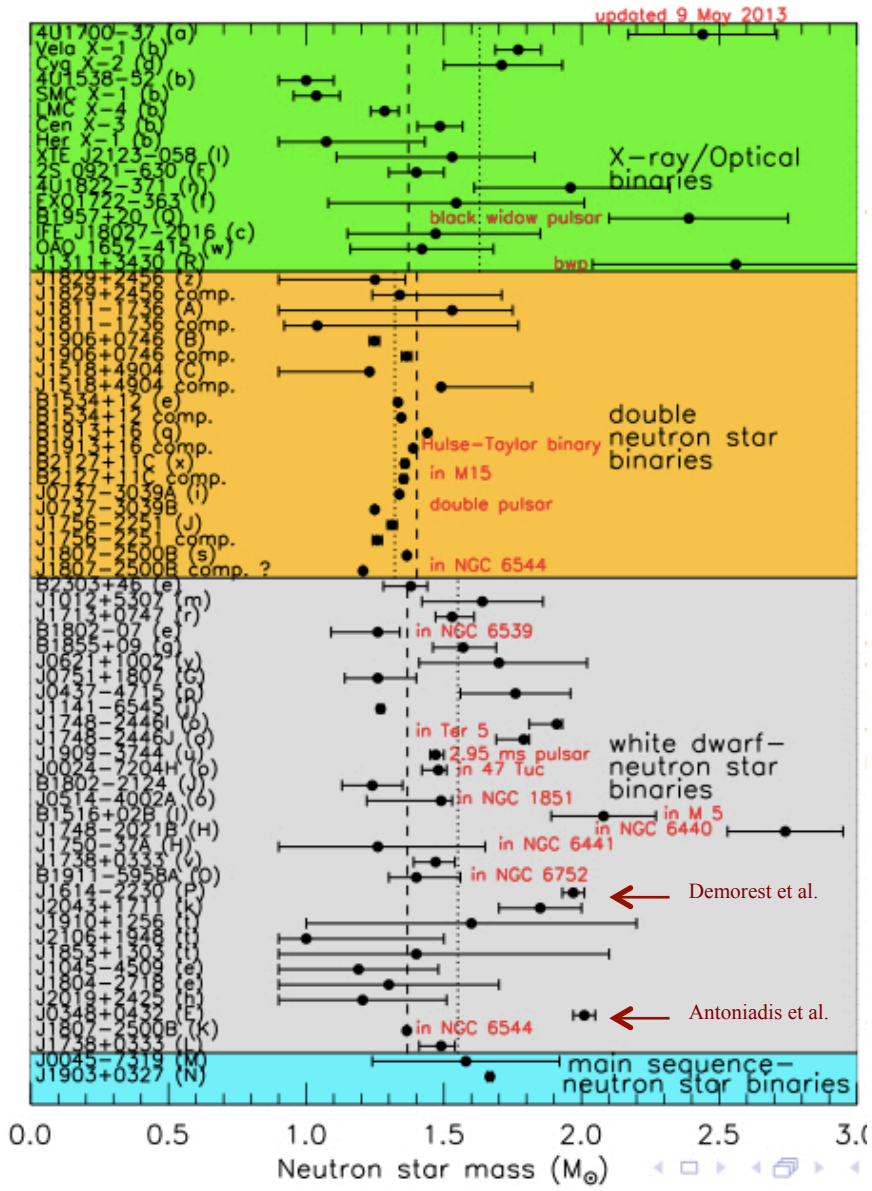

updated from Lattimer 2013

Observation of ~ 2 $M_\odot$ neutron stars imposes a very stringent constraint

Any reliable nuclear EoS should satisfy

$$M_{\max}[EoS] > 2M_\odot$$

otherwise is rule out

EoS Constraints from Neutron Star Radius

✧ **Pressure-radius correlation**

The analysis of this correlation can put stringent constraints in $E_{sym}(\rho)$

$$P(\rho,\beta)=\frac{\rho^2}{3\rho_0}\left(L\beta^2+\left(K_0+K_{sym}\beta^2\right)\frac{\rho-\rho_0}{3\rho_0}+\cdots\right)$$

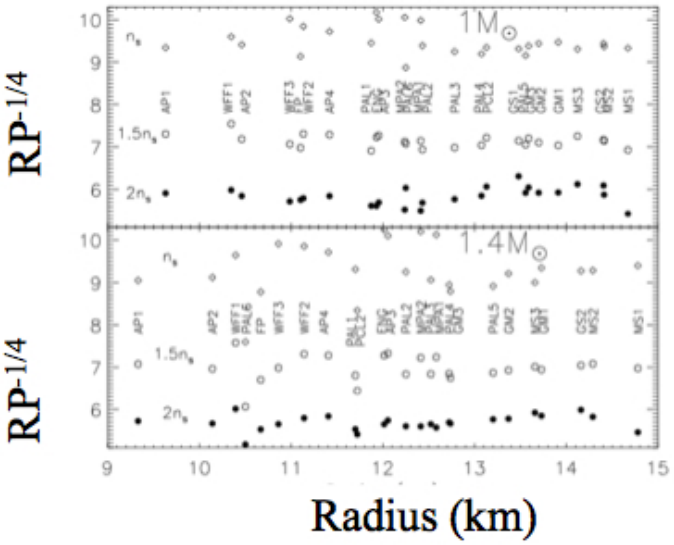

Lattimer & Prakash, ApJ 550, 426 (2001)

✧ **Low mass neutron stars**

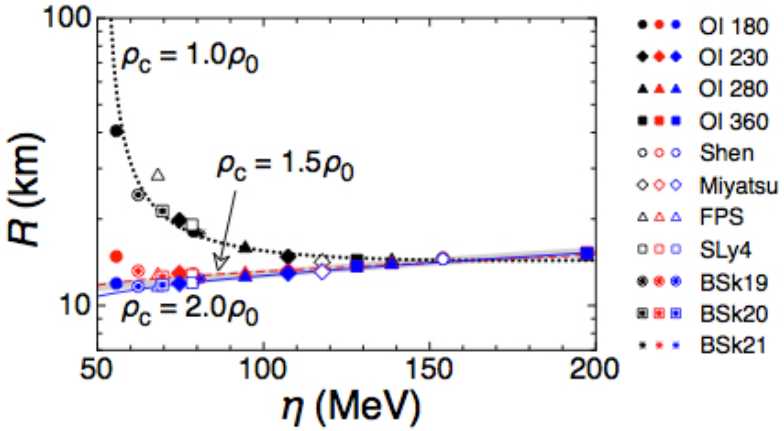

Possible simultaneous measurement of M & R of low mass NS could constrain EoS

$$\eta=\left(K_0L^2\right)^{1/3}$$

Sotani et al., PTEP 051E018 (2014)

Neutron Star Radii

Radii are very difficult to measure because NS:

- ✧ are very small (~ 10 km)
- ✧ are far from us (e.g., the closest NS, RX J1856.5-3754, is at ~ 400 ly)

A possible way to measure it is to use the thermal emission of low mass X-ray binaries:

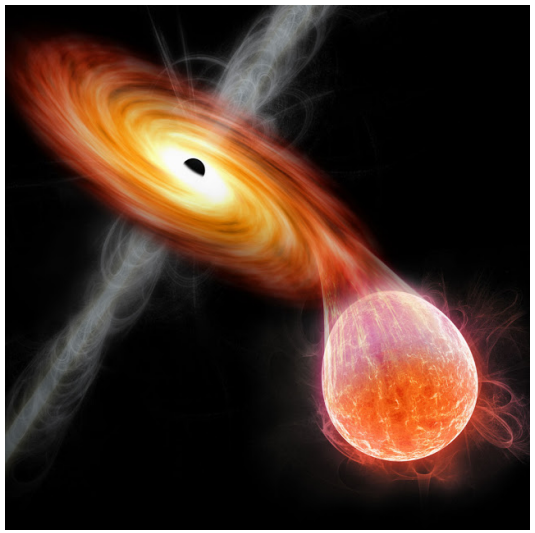

NS radius can be obtained from

- ✧ Flux measurement +Stefan-Boltzmann's law
- ✧ Temperature (Black body fit+atmosphere model)
- ✧ Distance estimation (difficult)
- ✧ Gravitational redshift z (detection of absorption lines)

$$R_\infty = \sqrt{\frac{FD^2}{\sigma_{SB}T^4}} \rightarrow R_{NS} = \frac{R_\infty}{1+z} = R_\infty \sqrt{1-\frac{2GM}{R_{NS}c^2}}$$

Recent Estimations of Neutron Star Radii

The recent analysis of the thermal spectrum from 5 quiescent LMXB in globular clusters is still controversial

Steiner et al. (2013, 2014)

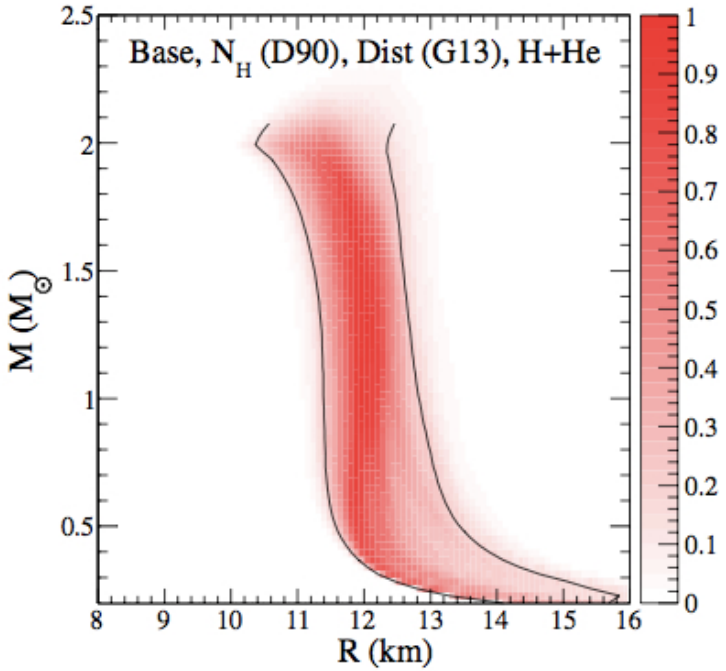

$$R = 12.0 \pm 1.4 km$$

Guillot et al. (2013, 2014)

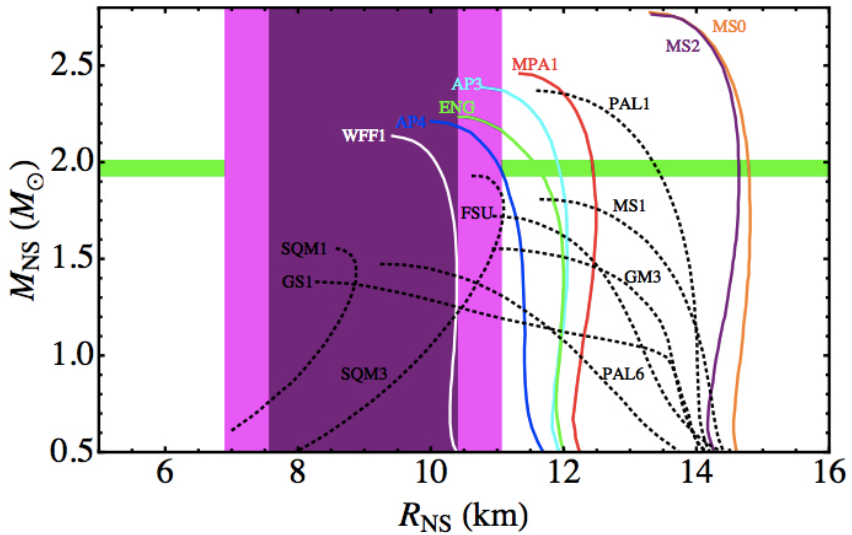

$$R = 9.1^{+1.3}_{-1.5} km \quad \text{2013 analysis}$$

$$R = 9.4 \pm 1.2 km \quad \text{2014 analysis}$$

NICER: Neutron Star Interior Composition Explorer

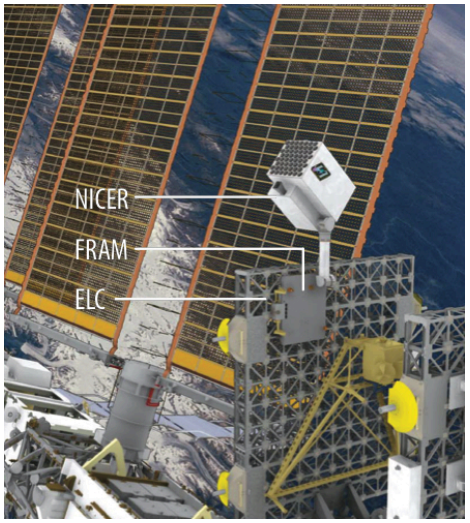

- ✧ International Space Station (ISS) payload devoted to the study of neutron stars through soft X-ray timing
- ✧ Launched aboard a SpaceX Falcon 9 rocket on June 3rd 2017

✧ Science objectives:

- ➢ To resolve the nature of ultradense matter at the threshold of collapse to a black hole
- ➢ To reveal the interior composition, dynamic processes & radiation mechanisms of neutron stars
- ➢ To measure neutron star radii to 5% precision

Neutron Star Rotation

Rotation of pulsars can be accurately measured. However, pulsars cannot spin arbitrarily fast. There is an absolute maximum (minimum) rotational frequency (period)

Centrifugal Force = Gravitational Force

⬇

Keplerian Frequency Ω_K
(EoS dependent)

Newtonian Gravity

$$P_{\min} = 2\pi\sqrt{\frac{R^3}{GM}} \approx 0.55\left(\frac{M_{sun}}{M}\right)^{1/2}\left(\frac{R}{10km}\right)^{3/2} \quad ms$$

General Relativity

$$P_{\min} = 0.96\left(\frac{M_{sun}}{M}\right)^{1/2}\left(\frac{R}{10km}\right)^{3/2} \quad ms$$

An observed frequency above the Ω_k predicted by a given EoS would rule out that model

Fasted pulsar known: PSR J1748-2446ad (P=1.39595482 ms)
cannot allow to put stringent constraints on existing EoS

Thermal Evolution of Neutron Stars

Information, complementary to that from mass & radius, can be also obtained from the measurement of the temperature (luminosity) of neutron stars

Two cooling regimes

Slow	Fast
Low NS mass	High NS mass

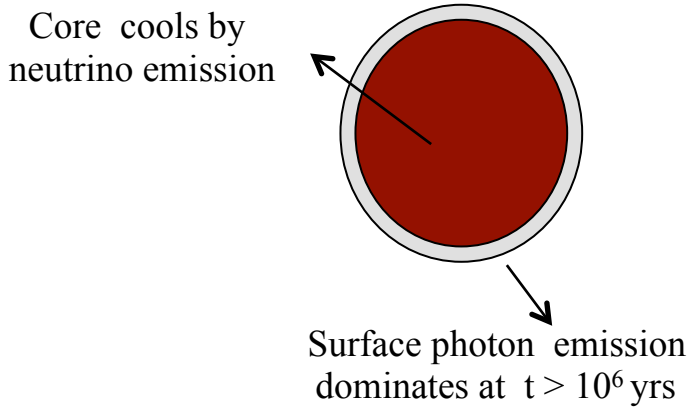

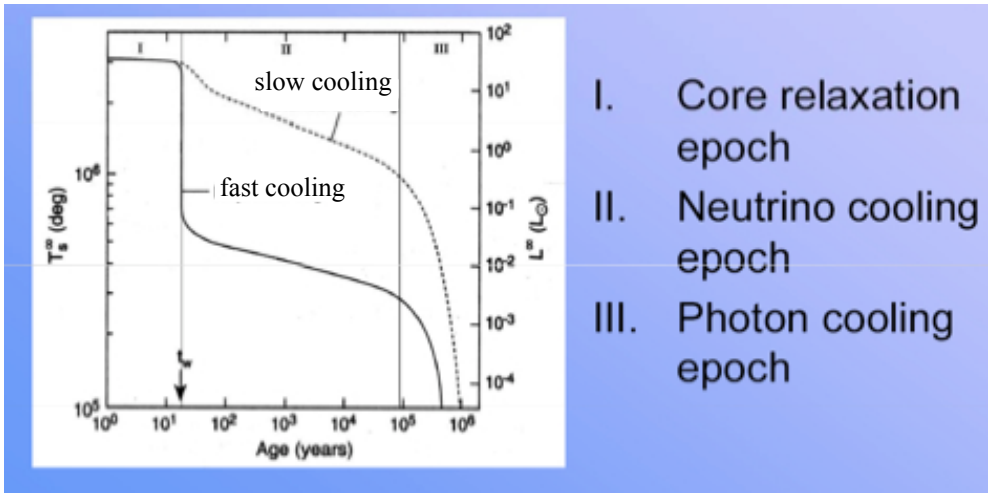

I. Core relaxation epoch
II. Neutrino cooling epoch
III. Photon cooling epoch

$$\frac{dE_{th}}{dt} = C_v \frac{dT}{dt} = -L_\gamma - L_\nu + H$$

- ✓ C_v: specific heat
- ✓ L_γ: photon luminosity
- ✓ L_ν: neutrino luminosity
- ✓ H: "heating"

Strong dependence on the NS composition & EoS

Multi-messenger Observations of the Event GW170817

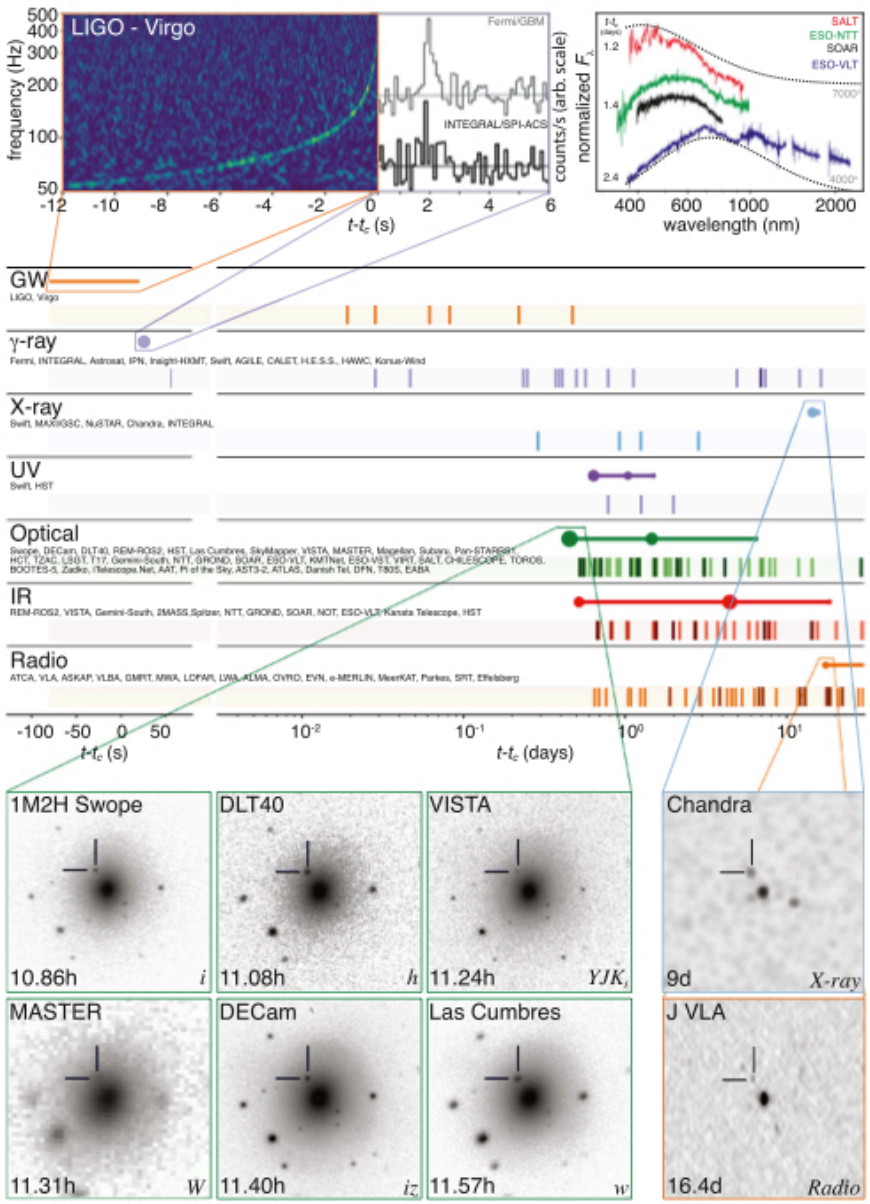

LIGO/VIRGO GW detection with associated electromagnetic events observed by over 70 observatories

- August 17th 2017 12:41:04 UTC

  GW from a BNS merger detected by Adv. LIGO & Adv. VIRGO

- + 1.7 seconds

  GRB (GRB170817A) detected by FERMI γ-ray Burst Monitor & INTEGRAL

- Next hours & days

  - New bright source of optical light (SSS17a) detected in the galaxy NGC 4993 in the Hydra constellation (+10h 52m)
  - Infrared emission observed (+11h 36m)
  - Bright ultraviolet emission detected (+15h)
  - X-ray emission detected (+9d)
  - Radio emission detected (+16d)

First Analysis & Implications of GW170817

The very first analysis of the event GW170817 seem to indicate:

- NS radii should be R < 13 km or even smaller than 12 km. Some analysis suggest R < 11 km ⟶ **Constraint on the EoS: those predicting large radii excluded ?**

- Low value of the upper limit of tidal deformability indicates a **soft EoS**

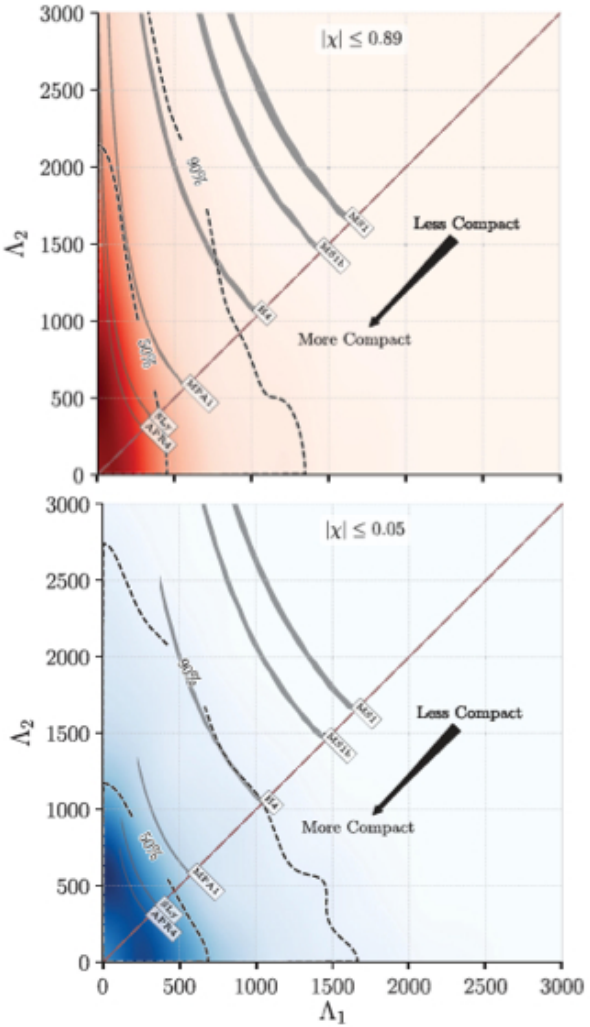

Other neutron star observables

Other NS observables can also help to constraint direct or indirectly the nuclear EoS

✧ Gravitational Redshift:

$$z = \left(1 - \frac{2GM}{c^2 R}\right)^{-1/2} - 1$$

Measurements of z allow to constraint the ratio of M/R

✧ Quasi-periodic Oscillations:

QPO in X-ray binaries measure the difference between the NS rot. freq. & the Keplerian freq. of the innermost stable orbit of matter elements in the accretion disk. Their observation & analysis can put stringent constraints on masses, radii & rotational periods

✧ NS moment of inertia:

$$I = \frac{J(\Omega)}{\Omega}; \quad J(\Omega) = \frac{8\pi}{3}\int_0^R dr r^4 \frac{p(r)+\varepsilon(r)}{\sqrt{1-\frac{2M(r)}{r}}}\left(\Omega - \omega(r)\right)e^{-\nu(r)}$$

Measurements of I could also constraint EoS. But not measured yet. Lower bound can be inferred from timing observations of Crab pulsar

Astrophysical determination of the nuclear EoS

- SLy below ρ_0
- Piecewise polytropic EoS above ρ_0 from mass-radius relation of 3 type-I X-ray bursts

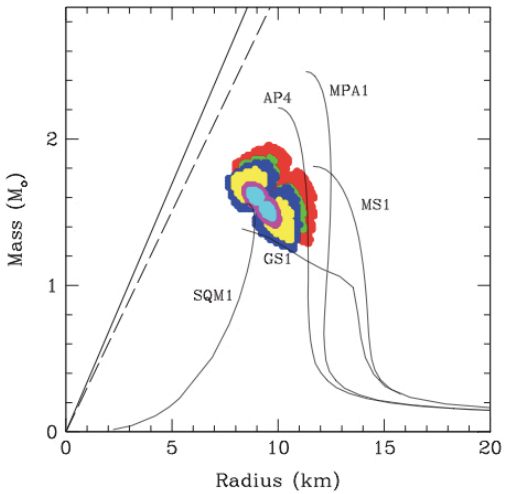

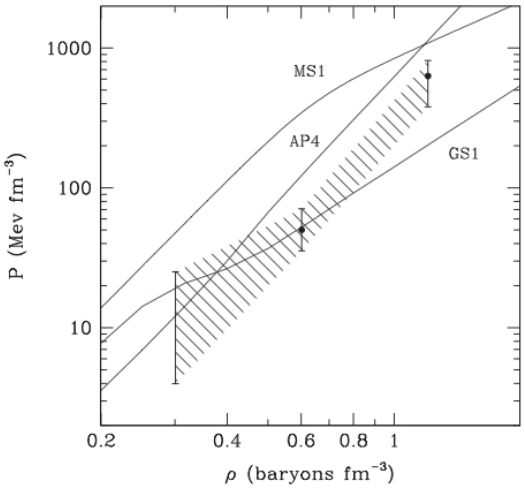

$$\rho_{i-1} < \rho \le \rho_i, \quad \varepsilon = \alpha_i \rho + \beta_i \rho^{\Gamma_i}, \quad P = \left(\Gamma_i - 1\right)\beta_i \rho^{\Gamma_i}$$

$\log P_0$ ($0.37\rho_{ns}$)	$\log P_1$ ($1.85\rho_{ns}$)	$\log P_2$ ($3.7\rho_{ns}$)	$\log P_3$ ($7.4\rho_{ns}$)
-0.64	[0.6–1.4]	$1.70^{+0.15}_{-0.15}$	$2.8^{+0.1}_{-0.2}$

F. Ozel & D. Psaltis, PRD 80, 103003 (2009)
F. Ozel, G. Baym & T. Guver, PRD 82, 101301(R) (2010)

Astrophysical determination of the nuclear EoS

✧ Nuclear parameters determined in a Bayesian data analysis of:

- 3 type-I X-ray burst
- 3 transient low mass X-ray binaries
- Cooling of 1 isolated NS, RX J1856-3754

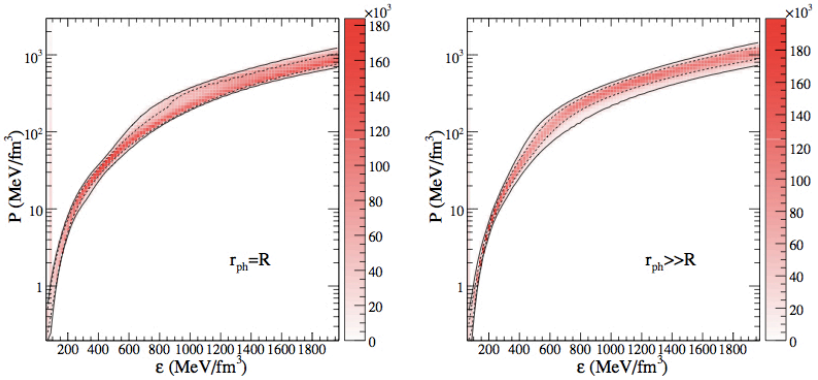

Parameters in the range expected from nuclear systematics & lab. experiments

Quantity	Lower Limit	Upper Limit
K (MeV)	180	280
K' (MeV)	−1000	−200
S_v (MeV)	28	38
γ	0.2	1.2
n_1 (fm^{-3})	0.2	1.5
n_2 (fm^{-3})	0.2	2.0
ε_1 (MeV fm^{-3})	150	600
ε_2 (MeV fm^{-3})	ε_1	1600

$$\varepsilon = n_B\left\{m_B + B + \frac{K}{8}(u-1)^2 + \frac{K'}{162}(u-1)^3 + (1-2x)^2\left[S_k u^{2/3} + S_p u^{\gamma}\right] + \frac{3}{4}\hbar c x\left(3\pi^2 n_b x\right)^{1/3}\right\}$$

$$u = \frac{n_B}{n_0}, \quad x = \frac{n_p}{n_B}$$

A. W. Steiner, J. M. Lattimer & E. F. Brown, ApJ 722, 33 (2010)

Building the Nuclear EoS

Approaches to the Nuclear EoS: "Story of Two Philosophies"

Ab-initio Approaches

Based on two- & three-nucleon realistic interactions which reproduce scattering data & the deuteron properties. The EoS is obtained by "solving" the complicated many-body problem

- Variational approaches: FHNC
- Diagrammatic: methods: BBG (BHF), SCGF
- Monte-Carlo techniques: VMC, DMC, GMC, AFDMC
- RG methods: $V_{low\ k}$
- Others: χEFT, Lattice Methods, High density perturbative QCD, DS approach

Phenomenological Approaches

Based on effective density-dependent interactions with parameters adjusted to reproduce nuclear observables & compact star properties.

- Non-relativistic: Skyrme & Gogny
- Relativistic: RMF
- Other: QMC, BCPM EDP

Non-homogeneous matter

- SN approximation models: Liquid drop models, TF models, Self-consistent models
- NSE models: NSE, Virial EoS, models with in-medium mass shifts

Difficulties of ab-initio approaches

- Different NN potentials in the market … but all are phase-shift equivalent

- Short range repulsion makes any perturbation expansion in terms of V meaningless. Different ways of treating SRC

- Complicated channel & operatorial structure (central, spin-spin, spin-isospin, tensor, spin-orbit, …)

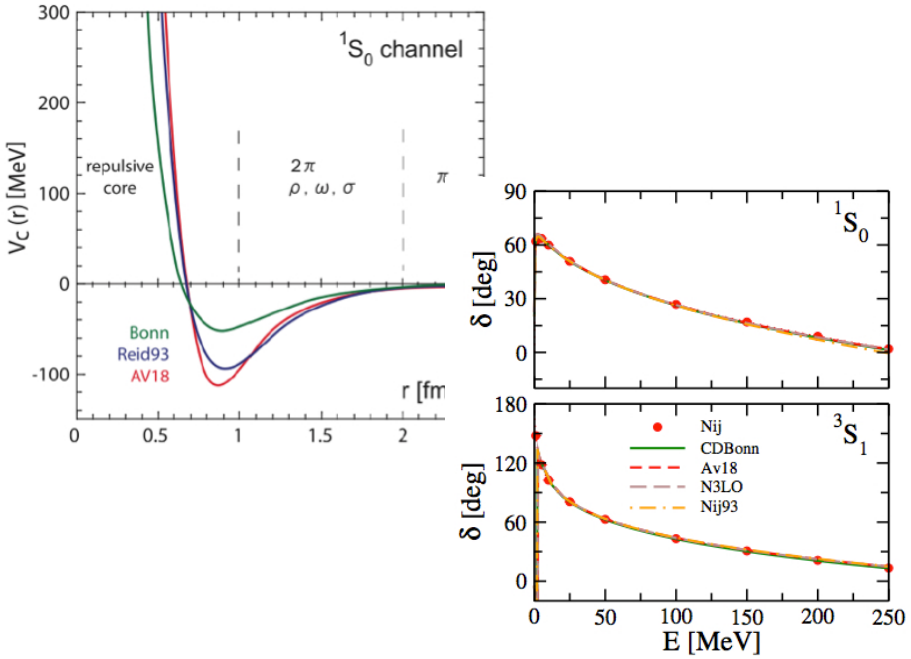

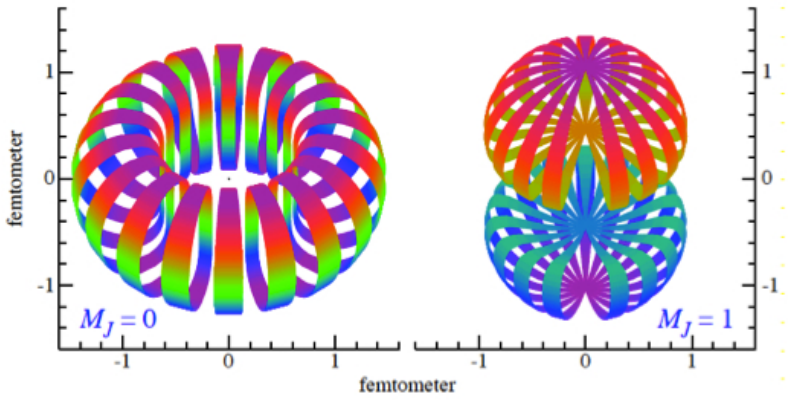

The NN interaction: meson exchange & potential models

✧ Meson Exchange Models:

NN interaction mediated by the exchange of different meson fields (e.g, Bonn, Nijmegen)

- ✧ scalar: σ, δ $\quad \Gamma_s = 1$
- ✧ pseudocalar: π, K, η $\quad \Gamma_{ps} = i\gamma^5$
- ✧ vector: ρ, K, ω, ϕ $\quad \Gamma_v = \gamma^\mu, \quad \Gamma_T = \sigma^{\mu\nu}$

$$L = g_M \Gamma_M \left(\bar{\Psi}_B \Psi_B\right) \phi_M$$

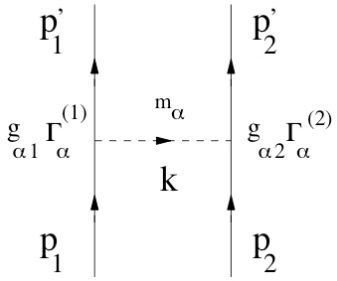

$$\left\langle p_1' p_2' \middle| V_M \middle| p_1 p_2 \right\rangle = \bar{u}(p_1') g_M^{(1)} \Gamma_M^{(1)} u(p_1) \frac{P_M}{(p_1 - p_1')^2 - m_M^2} \bar{u}(p_2') g_M^{(2)} \Gamma_M^{(2)} u(p_2)$$

Machleidt et al., PR. 149, 1 (1987)
Nagels et al., PRD 17, 768 (1978)

✧ Potential Models:

NN interaction is given by the sum of several local operators (e.g., Urbana, Argonne)

$$V_{ij} = \sum_{p=1,18} V_p(r_{ij}) O_{ij}^p$$

Ex: Local operators of Av18 potential

$$O_{ij}^{p=1,14} = \left[1, (\vec{\sigma}_i \cdot \vec{\sigma}_j), S_{ij}, \vec{L}\cdot\vec{S}, L^2, L^2(\vec{\sigma}_i \cdot \vec{\sigma}_j), (\vec{L}\cdot\vec{S})^2\right] \otimes \left[1, (\vec{\tau}_i \cdot \vec{\tau}_j)\right]$$

$$O_{ij}^{p=15,18} = \left[T_{ij}, (\vec{\sigma}_i \cdot \vec{\sigma}_j) T_{ij}, S_{ij} T_{ij}, (\tau_{zi} + \tau_{zj})\right]$$

Wiringa et al., PRC 51, 38 (1995)

Three-Nucleon Forces

Necessary to:

- ✧ Reproduce the spectra of light nuclei
- ✧ Saturate properly in non-relativistic many-body calculations

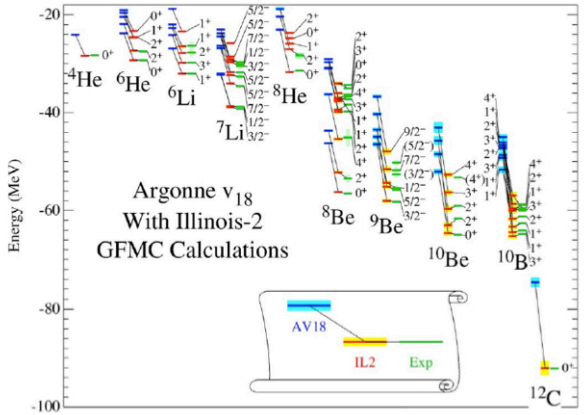

Pieper & Wiringa, ARNPS 51, 53 (2001)

✧ **Urbana-type** $V_{ijk}^{UIX} = V_{ijk}^{2\pi} + V_{ijk}^{R}$

$V_{ijk}^{2\pi}$: Attractive Fujita-Miyazawa force

V_{ijk}^{R} : Repulsive & Phenomenological

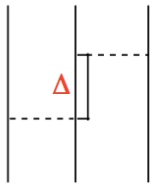

✧ **Microscopic-type**

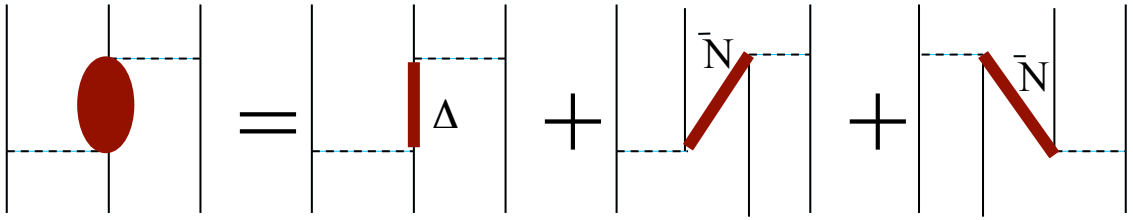

Problem: NNN is not independent of NN

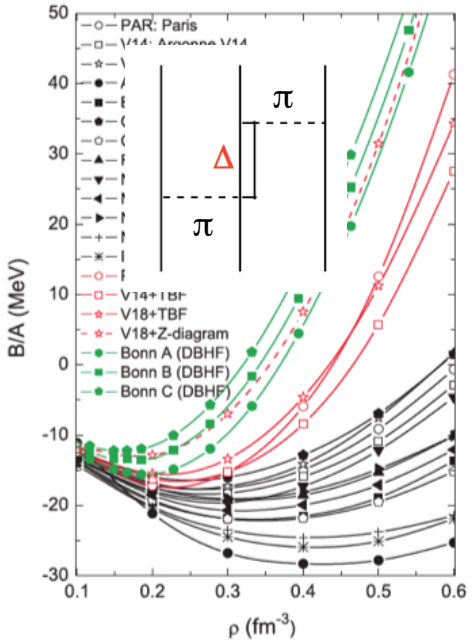

Li et al., PRC 74, 047304 (2006)

The NN interaction: χEFT forces

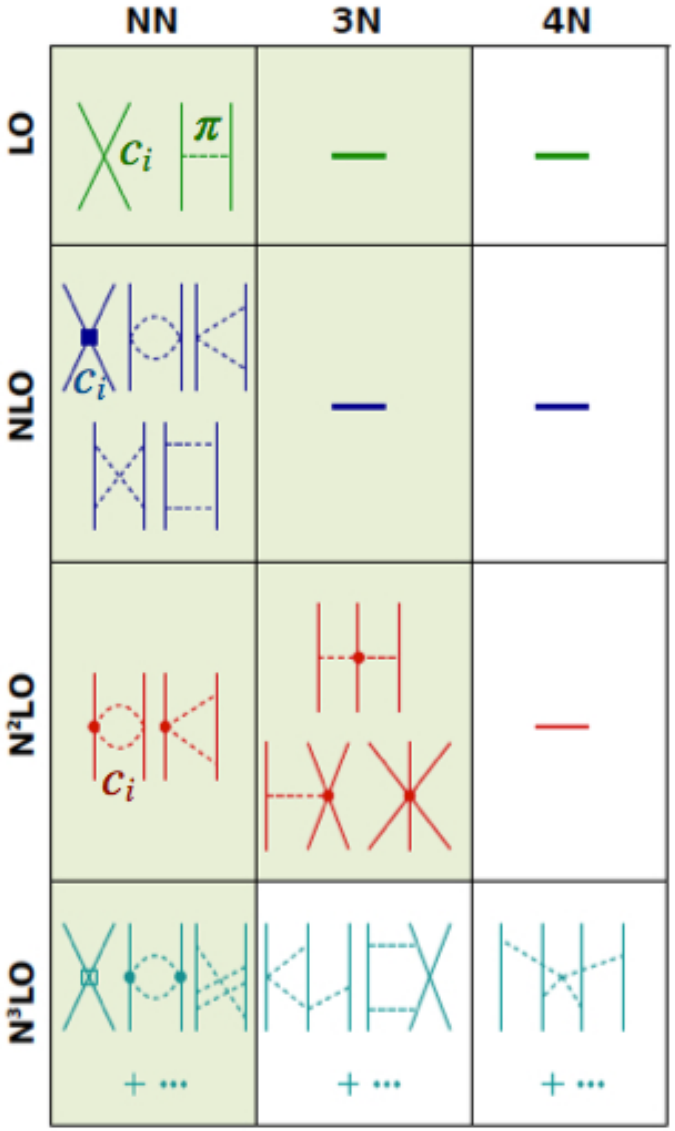

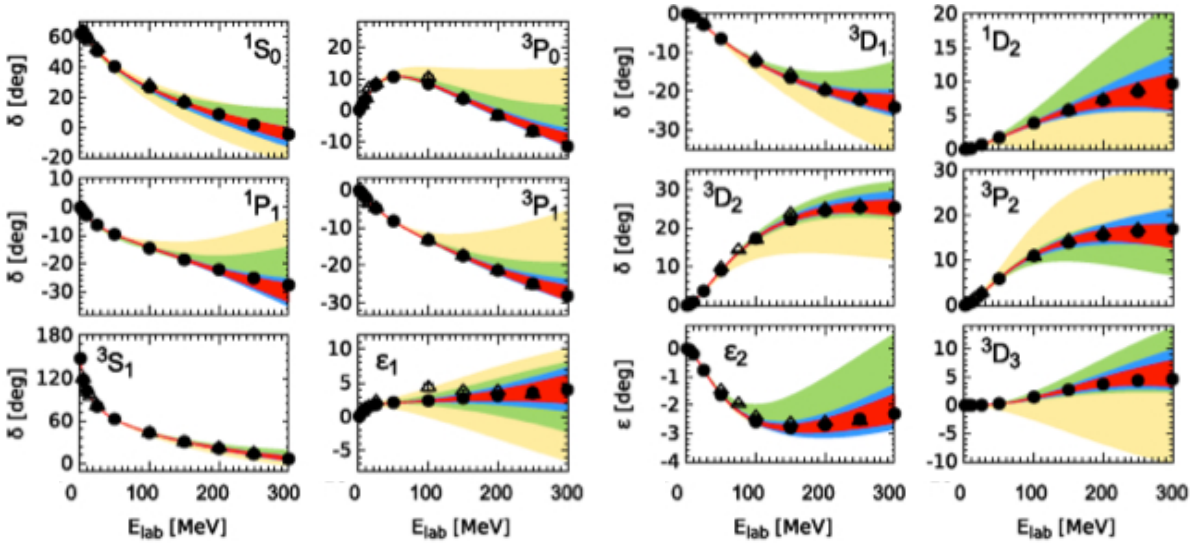

- ✧ Starting point: most general effective chiral Lagrangian that respect required QCD symmetries where π & N (recently also Δ) are the relevant d.o.f. of the theory
- ✧ Systematic expansion in powers of Q/Λ_χ [$Q=m_\pi$, k; $\Lambda_\chi \sim 1$ GeV]
- ✧ Consistent derivation of 2N, 3N, 4N, … forces

Weinberg, PLB 251, 288 (1990); NPB 363, 3 (1991)
Entem & Machleidt, PRC 68, 041001(R) (2003)
Epelbaum et al., NPA 747, 363 (2005)

Variational Approaches

Based on the variational principle

$$E \le \min\left\{\frac{\langle\Psi_T|\hat{H}|\Psi_T\rangle}{\langle\Psi_T|\Psi_T\rangle}\right\}, \quad |\Psi_T\rangle = \hat{F}|\Phi\rangle, \quad \hat{F} = \prod_{i>j}\sum_p f^{(p)}(r_{ij})\hat{O}_{ij}^{(p)}$$

correlation operator — uncorrelated w.f.

✧ Radial functions $f^{(p)}(r_{ij})$ are determined through functional minimization of the energy obtained using techniques like FHNC or VMC

FHNC: Integral equation method where the energy is evaluated by suming up series of clusters diagrams associated with the distribution functions of the many-body w.f. However:

- ✓ The sum is incomplete. Some topologies & operatorial structures are difficult to include (e.g., elementary diagrams)
- ✓ Spin-orbit correlations cannot be chained and are usually evaluated at the three-body cluster level

Second order perturbative corrections calculated in the CBF framework can be added.

Few nodal diagrams in FHNC

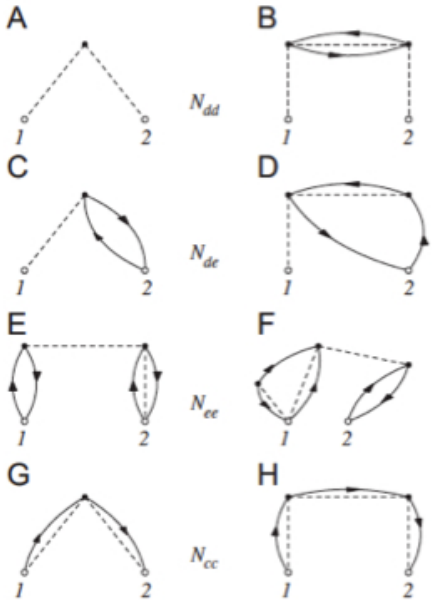

Fantoni & Rosati, Nuo. Cim. 25A, 593 (1975)

Diagrammatic Approaches: BBG theory

Ground state energy of nuclear matter evaluated in terms of the hole-line expansion (perturbative diagrams grouped according to the number of independent hole lines.)

- ✓ Hole-line expansion = expansion in ρ
- ✓ Contribution of diagram with h hole-lines to E/A $\propto \rho^{h-1}$
- ✓ Nuclear matter is a dilute system $c / r_0 < 1$

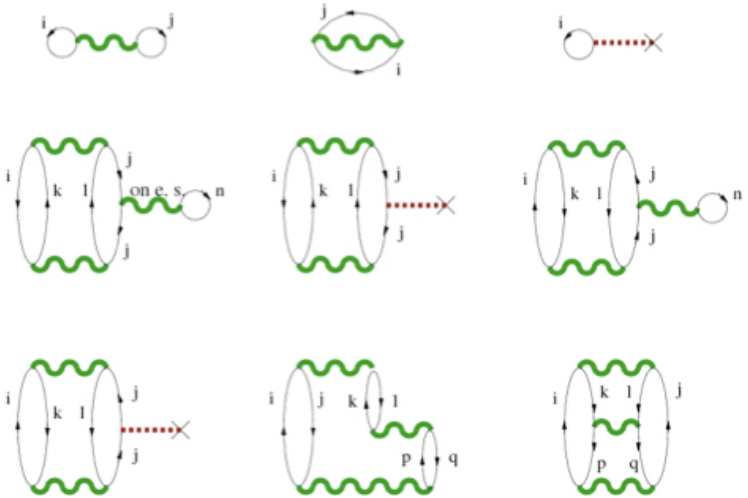

✧ Hole-line expansion derived by means of Brueckner's reaction matrix (G-matrix)

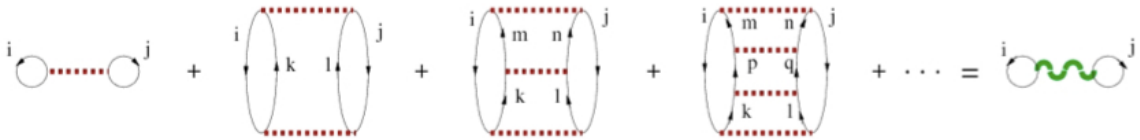

$$G(\omega) = V + V\frac{Q}{\omega - E - E' + i\eta}G(\omega)$$

✧ BHF approximation: leading term of the hole-line

$$E_{BHF} = \sum_{i\le A}\langle\alpha_i|K|\alpha_i\rangle + \frac{1}{2}\mathrm{Re}\left[\sum_{i,j\le A}\langle\alpha_i\alpha_j|G(\omega)|\alpha_i\alpha_j\rangle\right]$$

Infinite sumation of two-hole line diagrams

Day, Rev. Mod. Phys. 39, 719 (1967)

Diagrammatic Approaches: SCGF formalism

Energy obtained from the Galitskii-Migdal-Koltum (GMK) sum rule

$$E = \frac{\nu}{\rho}\int \frac{d^3k}{(2\pi)^3}\int_{-\infty}^{\infty}\frac{d\omega}{2\pi}\frac{1}{2}\left\{\frac{\hbar^2k^2}{2m}+\omega\right\}A\left(\vec{k},\omega\right)f\left(\omega\right)$$

s. p. spectral function — FD distribution

✧ Spectral function

$$A(\vec{k},\omega) = \frac{-2\,\mathrm{Im}\,\Sigma(\vec{k},\omega)}{\left[\omega - \frac{\hbar^2k^2}{2m} - \mathrm{Re}\,\Sigma(\vec{k},\omega)\right]^2 + \left[\mathrm{Im}\,\Sigma(\vec{k},\omega)\right]^2}$$

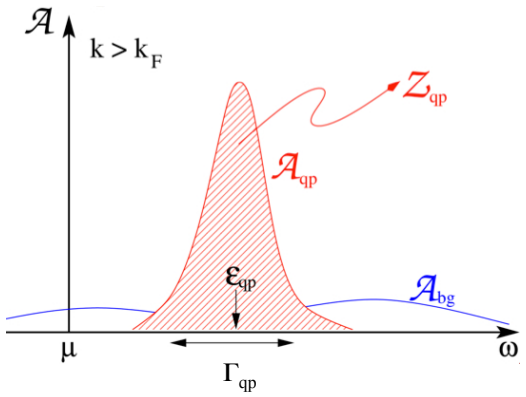

✧ Self-consistent computation scheme

In-medium interaction — Ladder self-energy — Dyson equation — Free two-particle propagator

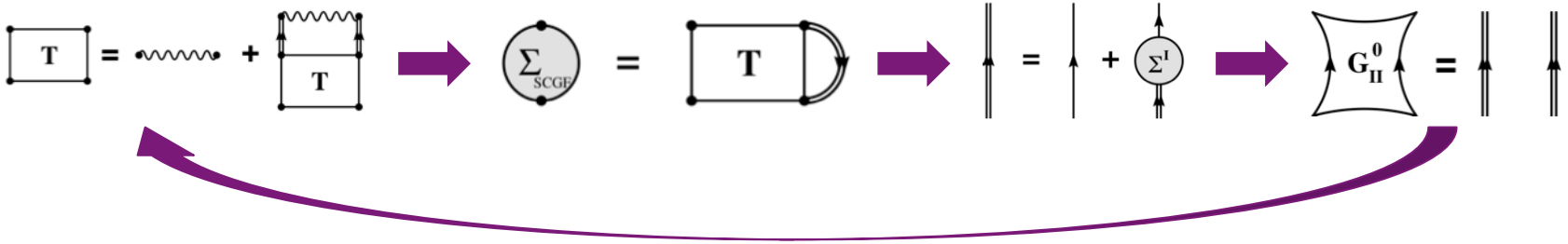

Figures adapted from A. Rios

Carbone et al., PRC 88, 054326 (2013)

Quantum Monte-Carlo Techniques

✧ VMC:

Evaluate energy & other observables using the Metropolis method

$$\langle \hat{O} \rangle = \frac{\sum_i \langle \Psi(\vec{R}_i) | \hat{O} | \Psi(\vec{R}_i) \rangle / W(\vec{R}_i)}{\sum_i \langle \Psi(\vec{R}_i) | \Psi(\vec{R}_i) \rangle / W(\vec{R}_i)}$$

Wiringa et al., PRC 62, 014001 (2000)

✧ DMC:

Model a diffusion process rewriting the Schoedinger equation in imaginary time

$$i\frac{\partial}{\partial t}|\Psi\rangle = \hat{H}|\Psi\rangle \Rightarrow -\frac{\partial}{\partial \tau}|\Psi\rangle = \hat{H}|\Psi\rangle$$

Anderson, J. Chem. Phys. 63, 1499 (19755)

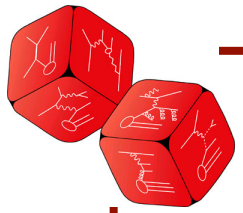

✧ GFMC:

Sample a trial wave function by evaluating path integrals of the form

$$|\Psi(\tau)\rangle = \prod \exp\left[-\left(\hat{H} - E_0\right)\Delta\tau\right]|\Psi_V\rangle$$

$$|\Psi(\tau)\rangle \underset{n\to\infty}{\rightarrow} |\Psi_0\rangle$$

Carlson et al., PRC 68, 025802 (2003)

✧ AFDMC:

Rewrite Green's function in order to change the quadratic dependence on spin & isospin operators to a linear one by introducing Hubbard-Stratonovich auxiliary fields

Gandolfi et al., PRC 79, 054005 (2009)

Low momentum NN interaction

Idea: start from a realistic NN interaction & integrate out the high momentum components

$V_{low\,k}$

- ✓ phase shift equivalent
- ✓ energy independent
- ✓ softer (no hard core)
- ✓ hermitian

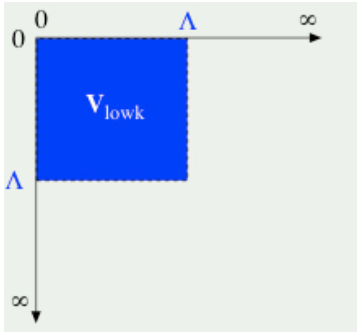

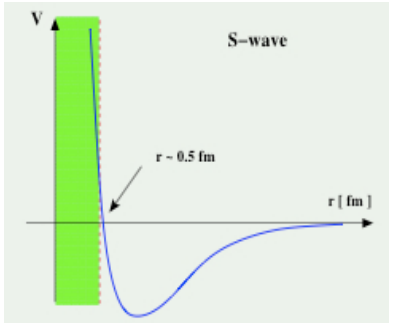

✧ Modified Lippmann-Schwinger Equation

$$T(k',k;E_k) = V_{low\,k}(k',k) + \frac{2}{\pi} P \int_0^\Lambda dq q^2 V_{low\,k}(k',q) \frac{1}{E_k - H_0(q)} T(q,k;E_k)$$

demanding $\frac{dT}{d\Lambda} = 0$

✧ Renormalization Group Flow Equation

$$\frac{d}{d\Lambda} V_{low\,k}(k',k) = -\frac{2}{\pi} \frac{V_{low\,k}(k',\Lambda) T(\Lambda,k;\Lambda^2)}{E_k - H_0(\Lambda)}$$

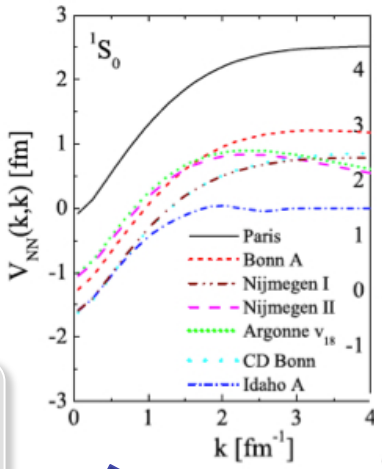

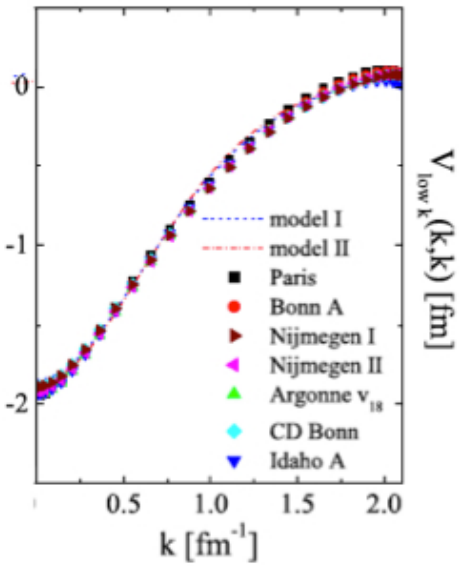

$V_{low\,k}$ evolved potentials

Bogner et al., Phys. Rep. 386, 1 (2003)

Other ab-initio approaches

✧ χEFT:

Chiral forces are usually used with standard many-body techniques. Recently, some effort have been devoted to develop an effective field theory directly for nuclear matter

Kaiser et al., NPA 697, 255 (2002); NPA 724, 47 (2003)

✧ Lattice methods:

Applied to light & medium mass nuclei and dilute neutron matter up to ~ $\rho_0/10$. No calculations of denser systems

e.g., Nuclear Lattice EFT

- ✓ Nucleons: point-like residing on lattice sites
- ✓ Interactions: EFT nuclear forces. Represented on lattice as insertions on nucleon world lines

Lee, Prog. Part. Nucl. Phys. 63, 117 (2009)

✧ High density Perturbative QCD:

Recent efforts aim to account for all second-order $O(\alpha_s^2)$ effects in an expansion of the thermodynamic pressure of deconfined QCD.

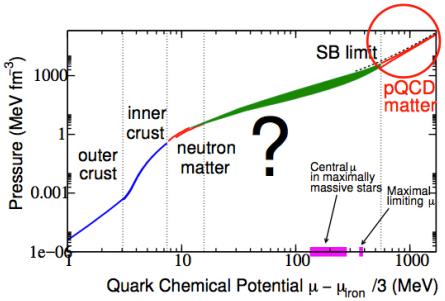

Kurkela et al., APJ 789, 127 (2014)

✧ Dyson-Schwinger approach:

Non-perturbative approach to analyze QCD. Starting point: QCD partition function from which integral DS equations are derived for the n-point Scwhinger functions of the theory. Recently used to compute the EoS of dense homogeneous quark matter in the deconfined phase

Chen et al., PRD 78, 116015 (2008)

A comparison of some ab-initio approaches

Compare different many-body techniques using the same NN interaction (Argonne family) to find the sources of discrepancies & ultimately determine "systematic error" associated to the nuclear EoS predicted predicted by many-body theory

Symmetric nuclear matter

Pure neutron matter

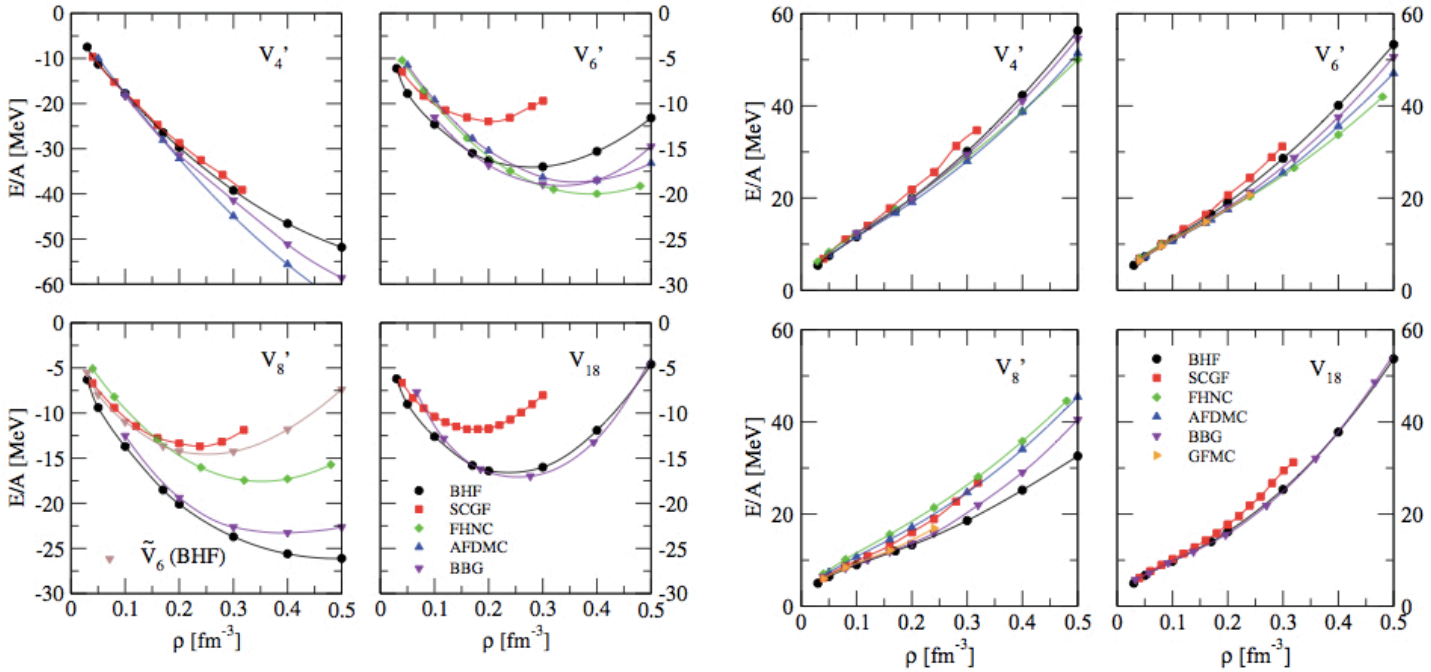

Tensor & spin-orbit and their in-medium treatment are at the heart of most of the observed discrepancies

M. Baldo, A. Polls, A. Rios, H.-J. Schulze & I.Vidaña, PRC 86, 064001 (2012)

Phenomenological Models: Skyrme & Gogny interactions

✧ Skyrme interactions:

Effective zero-range density dependent interaction

$$\hat{V}(\vec{r}_1,\vec{r}_2) = t_0\left(1+x_0\hat{P}_\sigma\right)\delta(\vec{r}_{12}) + \frac{t_1}{2}\left(1+x_1\hat{P}_\sigma\right)\left[\hat{k}'\delta(\vec{r}_{12}) + \delta(\vec{r}_{12})\hat{k}^2\right]$$
$$+t_2\left(1+x_2\hat{P}_\sigma\right)\hat{k}'\delta(\hat{r}_{12})\hat{k} + \frac{t_3}{6}\left(1+x_3\hat{P}_\sigma\right)\rho^\alpha(\vec{R}_{12})\delta(\hat{r}_{12})$$
$$+iW_0\left(\hat{\sigma}_1+\hat{\sigma}_2\right)\left[\hat{k}'\times\delta(\hat{r}_{12})\hat{k}\right]$$

Evaluation of the energy density in the HF approximation yields for nuclear matter a simple EDF in fractional powers of the number densities. Many parametrizations exist

Skyrme, Nucl. Phys. 9, 615 (1959)

✧ Gogny interactions:

Effective finite-range density dependent interaction

$$\hat{V}(\vec{r}_1,\vec{r}_2) = \sum_{j=1,2}\exp\left(-\frac{r_{12}^2}{\mu_j^2}\right)\left(W_j + B_j\hat{P}_\sigma - H_j\hat{P}_\tau - M_j\hat{P}_\sigma\hat{P}_\tau\right)$$
$$+t_0\left(1+x_0\hat{P}_\sigma\right)\rho^\alpha(\vec{R}_{12})\delta(\hat{r}_{12})$$
$$+iW_0\left(\hat{\sigma}_1+\hat{\sigma}_2\right)\left[\hat{k}'\times\delta(\hat{r}_{12})\hat{k}\right]$$

Due to the finite-range terms the evaluation of the energy density is numerically more involved. Less number of parametrizations in the market

Brink & Boeker, NPA 91, 1 (1967)

Phenomenological Models: Relativistic Mean Field Models

Based in effective Lagrangian densities where the interaction is modeled by meson exchanges

$$L = L_{nuc} + L_{mes} + L_{\text{int}} + L_{nl}$$

$$L_{nuc} = \sum_{i=n,p} \bar{\psi}_i \left(\gamma_\mu i\partial^\mu - m_i \right) \psi_i$$

$$L_{mes} = \frac{1}{2}\left(\partial^\mu \sigma \partial_\mu \sigma - m_\sigma^2 \right) + \frac{1}{2}\left(\partial^\mu \vec{\delta} \partial_\mu \vec{\delta} - m_\sigma^2 \right) - \frac{1}{4} G_{\mu\nu} G^{\mu\nu} + \frac{1}{2} m_\omega^2 \omega_\mu \omega^\mu - \frac{1}{4} H_{\mu\nu} H^{\mu\nu} + \frac{1}{2} m_\omega^2 \vec{\rho}_\mu \cdot \vec{\rho}^\mu$$

$$L_{\text{int}} = -\sum_{i=n,p} \bar{\psi}_i \left[\gamma_\mu \left(g_\omega \omega^\mu + g_\rho \vec{\tau} \cdot \vec{\rho}^\mu \right) + g_\sigma \sigma + g_\delta \vec{\tau} \cdot \vec{\delta} \right] \psi_i$$

$$L_{nl} = -\frac{A}{3}\sigma^3 - \frac{B}{4}\sigma^4 + \frac{C}{4}\left(\omega_\mu \omega^\mu \right)^2 + D\left(\omega_\mu \omega^\mu \right)\left(\vec{\rho}_\mu \cdot \vec{\rho}_\mu \right)$$

Nucleon & meson equations of motion are derived from the Lagrangian density and usually self-consistently solved in the mean field approximation where mesons are treated as classical fields and negative-energy states of nucleons are neglected

Boguta & Bodmer, NPA 292, 413 (1977)

Serot & Walecka, Adv. Nuc. Phys. 16, 1 (1986)

Other phenomenological models

✧ Quark Meson Coupling model:

Closely related with the RMF. Nucleons are considered a bound states of quarks which couple with mesons in the surrounding medium

Downum et al., Phys. Lett. B 638, 455 (2006)

✧ Barcelona-Catania-Paris-Madrid EDF:

EDF constructed by parametrizing BHF results obtained with realistic NN interactions. The addition of appropiate surface & spin-orbit contributions proves an excellent description of finite nuclei

Baldo et al., PRC 87, 064305 (2013)

✧ Other:

- ✓ Density-dependent separable model (SMO)
- ✓ Three-range Yukawa (M3Y) interactions

Rikovska Stone, PRC 65, 064312 (2002)
Nakada, PRC 68, 014316 (2003)

A comparison of phenomenological models

Proliferation of phenomenological models predicting different SM & NM EoS

Skyrme

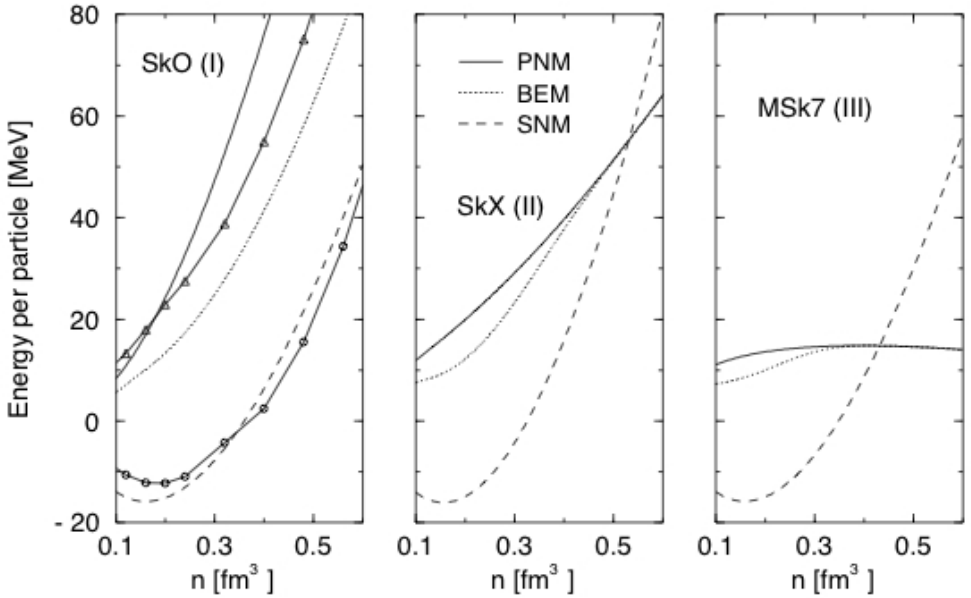

J. R. Stone et al., PRC 68, 034324 (2003)

RMF

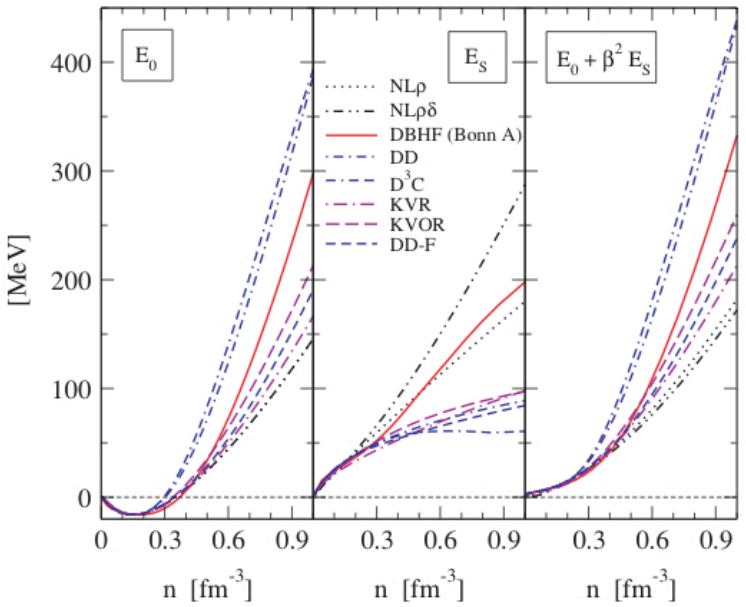

T. Klahn et al., PRC 74, 035802 (2006)

Recently M. Dutra et al., (PRC 90, 055203 (2014)) have analyzed 263 parametrizations of 7 different types of RMF imposing constraints from SM, PNM & Symmetry Energy and its derivatives. Similar analysis was done for 240 Skyrme forces by M. Dutra et al., (PRC 85, 035201 (2012)). In both cases a few number of parametrizations passed the stringent tests imposed

EoS for non-homogeneous nuclear matter

Non-uniform nuclear matter is present in the NS crust and SN cores (low ρ, low T). Till now only two types of phenomenological approaches have been used to describe it:

Single-nucleus approximation models

Composition of matter is assumed to be made of one representative heavy nucleus (the one energetically favored) + light nuclei (α particles) or unbound nucleons

- ✓ (Comprenssible) Liquid-Drop models
- ✓ (Extended) Thomas-Fermi models
- ✓ Self-consistent mean-field models

Nuclear Statistical Equilibrium models

Composition of matter is assumed to be a statistical ensemble of different nuclear species and nucleons in thermodynamical equilibrium

- ✓ (Extended) NSE
- ✓ Virial EoS
- ✓ Models with in-medium mass shifts

Hyperons: the strange ingredients of the nuclear EoS

What do we know to include hyperons in the nuclear EoS ?

Unfortunately, much less than in the pure nucleonic sector to put stringent constraints on the YN & YY interactions

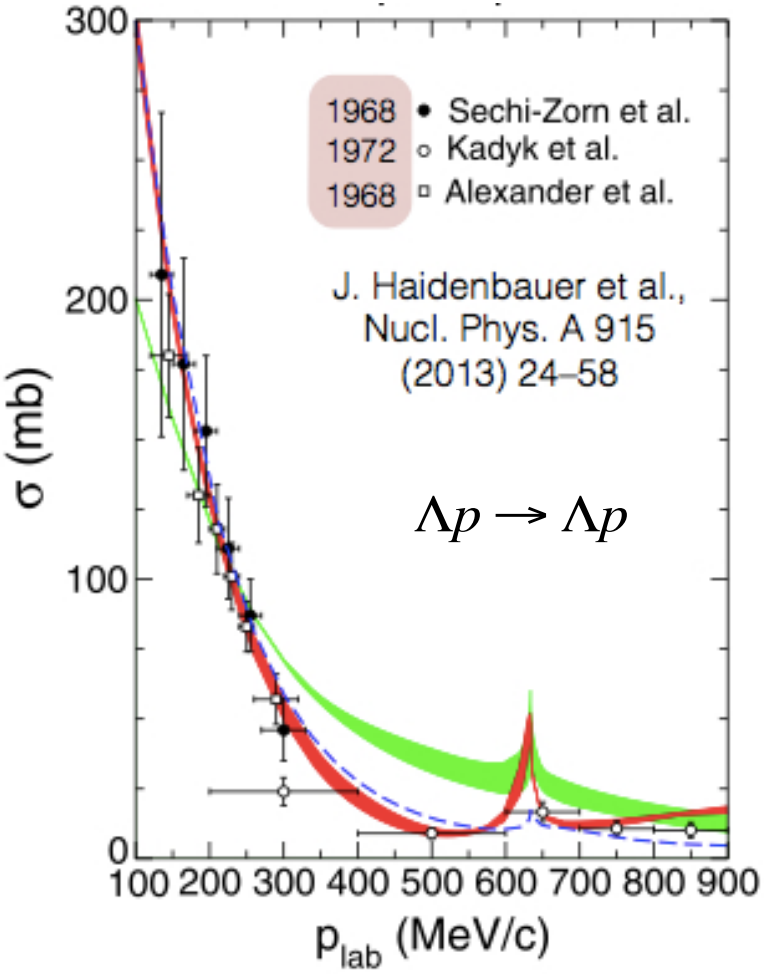

- Very few YN scattering data due to short lifetime of hyperons & low intensity beam fluxes
  - ~ 35 data points, all from the 1960s
  - 10 new data points, from KEK-PS E251 collaboration (2000)
- No YY scattering data exists

(cf. > 4000 NN data for $E_{lab} < 350$ MeV)

Hypernuclear Physics

Goal: Relate hypernuclear observables with the bare YN & YY interactions

- 41 single Λ-hypernuclei ⟶ ΛN attractive ($U_\Lambda(\rho_0) \sim -30$ MeV)
- 3 double-Λ hypernuclei ⟶ weak ΛΛ attraction ($\Delta B_{\Lambda\Lambda} \sim 1$MeV)
- Very few Ξ-hypernuclei ⟶ ΞN attractive ($U_\Xi(\rho_0) \sim -14$ MeV)
- Ambiguous evidence of Σ-hypernuclei ⟶ ΣN repulsive ($U_\Sigma(\rho_0) > +15$ MeV) ?

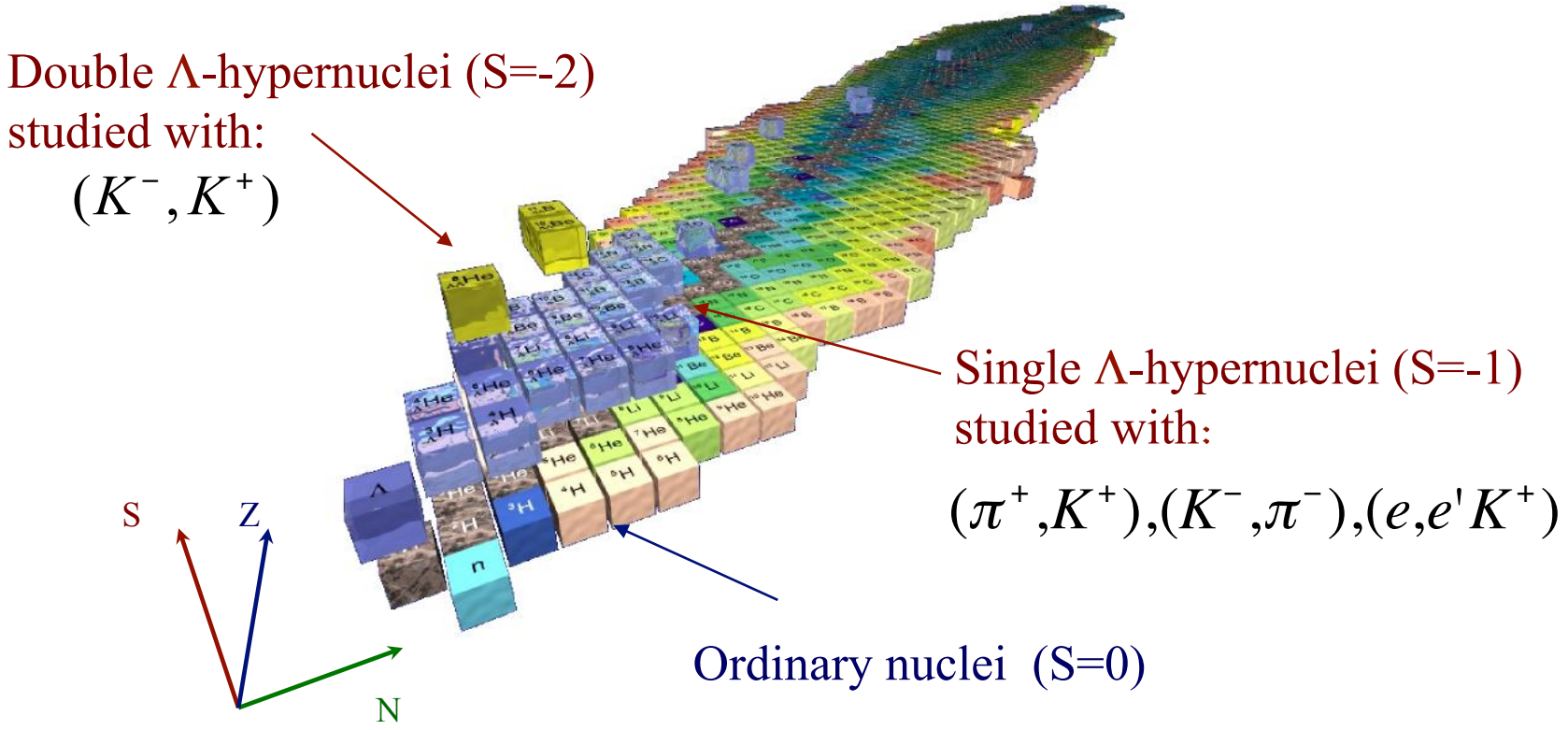

Unfortunately, there are always problems …

- Limited amount of scattering data not enough to fully constrain the bare YN & YY interactions ⟶ Strategy: start from a NN model & impose $SU(3)_f$ constraints to build YN & YY (e.g., Juelich & Nijmegen models)
- Bare YN & YY is not easy to derive from hypernuclei. Hyperons in nuclei are not free but in-medium. Hypernuclei provide effective hyperon-nucleus interactions
- Amount of experimental data on hypernuclei is not enough to constrain the uncertainties of phenomenological models. Parameters are most of the times arbitrarily chosen
- Ab-initio hypernuclear structure calculations with bare YN & YY interactions exists but are less accurate than phenomenological ones due to the difficulties to solve the very complicated nuclear many-body problem

Lattice QCD

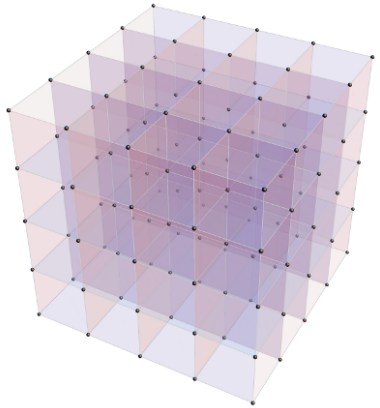

Lattice QCD calculations can provide the much required YN, YY & hyperonic TBFs

ΛN (I=0) $^1S_0$ (m_π=570 MeV)

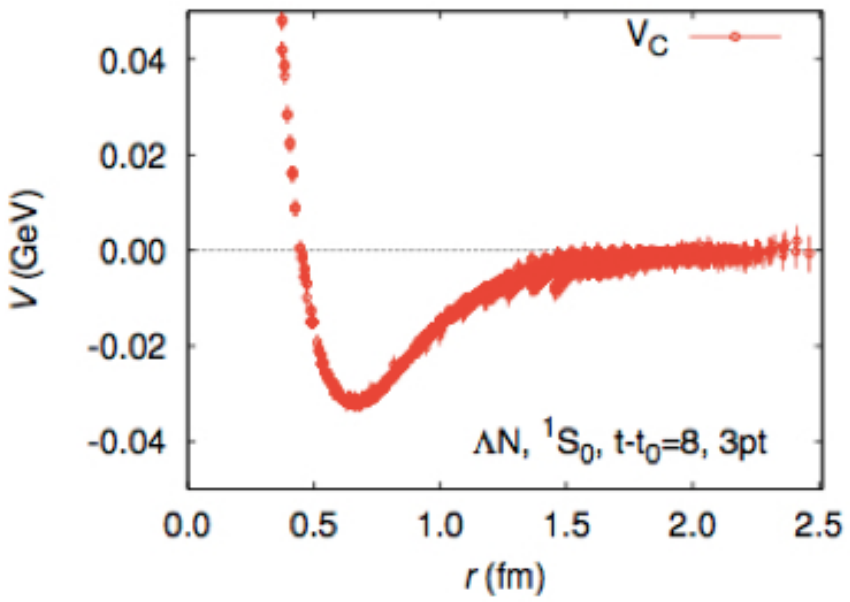

$\Lambda\Lambda$, $N\Xi$ & $\Sigma\Sigma$ (I=0) $^1S_0$ (m_π=145 MeV)

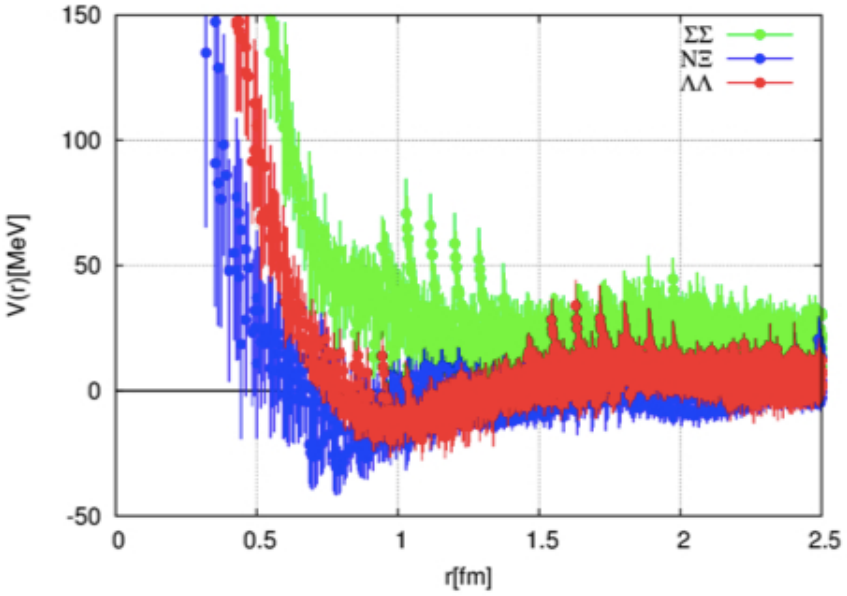

Hal QCD collaboration, HYP2015

The final message of this talk

- Major experimental, observational & theoretical advances on understanding the nuclear EoS have been done in the last decades & will be done in the near future
- The isoscalar part of the nuclear EoS is rather well constrained
- Why the isovector part is less well constrained is still an open question whose answer is probably related to our limited knowledge of the nuclear force and, particularly, of its spin & isospin dependence

- You for your time & attention
- The organizers for their invitation